



## Added-value of ensemble prediction system on the quality of solar irradiance probabilistic forecasts

Le Gal La Salle, Josselin; Badosa, Jordi; David, Mathieu; Pinson, Pierre; Lauret, Philippe

*Published in:*  
Renewable Energy

*Link to article, DOI:*  
[10.1016/j.renene.2020.07.042](https://doi.org/10.1016/j.renene.2020.07.042)

*Publication date:*  
2020

*Document Version*  
Peer reviewed version

[Link back to DTU Orbit](#)

*Citation (APA):*  
Le Gal La Salle, J., Badosa, J., David, M., Pinson, P., & Lauret, P. (2020). Added-value of ensemble prediction system on the quality of solar irradiance probabilistic forecasts. *Renewable Energy*, 162, 1321-1339. <https://doi.org/10.1016/j.renene.2020.07.042>

---

### General rights

Copyright and moral rights for the publications made accessible in the public portal are retained by the authors and/or other copyright owners and it is a condition of accessing publications that users recognise and abide by the legal requirements associated with these rights.

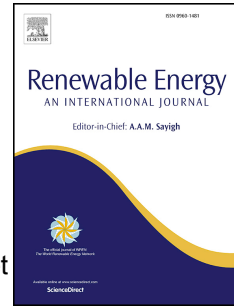
- Users may download and print one copy of any publication from the public portal for the purpose of private study or research.
- You may not further distribute the material or use it for any profit-making activity or commercial gain
- You may freely distribute the URL identifying the publication in the public portal

If you believe that this document breaches copyright please contact us providing details, and we will remove access to the work immediately and investigate your claim.

# Journal Pre-proof

Added-value of ensemble prediction system on the quality of solar irradiance probabilistic forecasts

Josselin Le Gal La Salle, Jordi Badosa, Mathieu David, Pierre Pinson, Philippe Lauret



PII: S0960-1481(20)31118-6

DOI: <https://doi.org/10.1016/j.renene.2020.07.042>

Reference: RENE 13873

To appear in: *Renewable Energy*

Received Date: 5 March 2020

Revised Date: 24 June 2020

Accepted Date: 10 July 2020

Please cite this article as: Le Gal La Salle J, Badosa J, David M, Pinson P, Lauret P, Added-value of ensemble prediction system on the quality of solar irradiance probabilistic forecasts, *Renewable Energy* (2020), doi: <https://doi.org/10.1016/j.renene.2020.07.042>.

This is a PDF file of an article that has undergone enhancements after acceptance, such as the addition of a cover page and metadata, and formatting for readability, but it is not yet the definitive version of record. This version will undergo additional copyediting, typesetting and review before it is published in its final form, but we are providing this version to give early visibility of the article. Please note that, during the production process, errors may be discovered which could affect the content, and all legal disclaimers that apply to the journal pertain.

© 2020 Published by Elsevier Ltd.

- Josselin LE GAL LA SALLE : Investigation, Methodology, Conceptualization, Data curation, Visualization, Software, Writing
- Mathieu DAVID : Methodology, Writing - original draft, review & editing
- Pierre PINSON : Methodology, review & editing
- Jordi BADOSA : Data curation, review & editing
- Philippe LAURET : Methodology, Project administration, Conceptualization, Writing, Validation, review & editing

# Added-value of Ensemble Prediction System on the quality of solar irradiance probabilistic forecasts

Josselin Le Gal La Salle<sup>a</sup>, Jordi Badosa<sup>b</sup>, Mathieu David<sup>a</sup>, Pierre Pinson<sup>c</sup>, Philippe Lauret<sup>a</sup>

<sup>a</sup>*Université de la Réunion - Laboratoire de Physique et ingénierie mathématique pour l'énergie, l'environnement et le bâtiment (PIMENT), 15 avenue René Cassin, 97715, Saint-Denis Cedex 9, La Réunion, France*

<sup>b</sup>*LMD-Laboratoire de météorologie dynamique, Palaiseau, France*

<sup>c</sup>*DTU - Technical University of Denmark*

---

## Abstract

Accurate solar forecasts is one of the most effective solution to enhance grid operations. As the solar resource is intrinsically uncertain, a growing interest for solar probabilistic forecasts is observed in the solar research community. In this work, we compare two approaches for the generation of day-ahead solar irradiance probabilistic forecasts. The first class of models termed as deterministic-based models generates probabilistic forecasts from a deterministic value of the irradiance predicted by a Numerical Weather Prediction (NWP) model. The second type of models denoted by ensemble-based models issues probabilistic forecasts through the calibration of an Ensemble Prediction System (EPS) or from information (such as mean and variance) derived from the ensemble. The verification of the probabilistic forecasts is made using a sound framework. A numerical score, the Continuous Ranked Probability Score (CRPS), is used to assess the overall performance of the different models. The decomposition of the CRPS into reliability and resolution provides a further detailed insight into the quality of the probabilistic forecasts. In addition, a new diagnostic tool which evaluates the contribution of the statistical moments of the forecast distributions to the CRPS is proposed. This tool denoted by MC-CRPS allows identifying the characteristics of an ensemble that have an impact on the quality of the probabilistic forecasts. The assessment of the different models is done on several sites experiencing very different climatic conditions. Results show a general superior performance of ensemble-based models as the gain in forecast quality measured by the CRPS ranges from 4% to 16% depending on the site.

*Keywords:* Day-ahead solar irradiance probabilistic forecast, Ensemble prediction system, Non parametric methods, Ensemble calibration, CRPS

---

## 1 Contents

### 2 1 Introduction

2

---

\*Fully documented templates are available in the elsarticle package on CTAN.

3	<b>2 Building probabilistic forecasts</b>	<b>5</b>
4	2.1 Statistical techniques used to generate probabilistic forecasts . . . . .	5
5	2.1.1 The linear quantile regression (LQR) technique . . . . .	5
6	2.1.2 The Analog Ensemble (AnEn) technique . . . . .	8
7	2.1.3 The Nonhomogeneous truncated Gaussian Regression technique ( $t\_NGR$ )	9
8	2.1.4 The Nonhomogeneous Regression of Generalized Extreme Value tech-	
9	nique ( $NR\_GEV$ ) . . . . .	9
10	2.2 Obtaining probabilistic forecasts from deterministic forecasts (Deterministic-	
11	based approach) . . . . .	11
12	2.3 Obtaining probabilistic forecasts from ensemble forecasts (Ensemble-based	
13	approach) . . . . .	11
14	2.3.1 From the raw output of ECMWF-EPS . . . . .	11
15	2.3.2 From information extracted from an EPS . . . . .	11
16	<b>3 Verification of the probabilistic forecasts</b>	<b>12</b>
17	3.1 Attributes for a skillful probabilistic model . . . . .	12
18	3.2 CRPS . . . . .	13
19	3.2.1 Definition . . . . .	13
20	3.2.2 CRPS Skill Score . . . . .	13
21	3.2.3 Decomposition of the CRPS . . . . .	14
22	3.3 Contributions of the statistical moments of the forecast distribution to the	
23	CRPS . . . . .	14
24	<b>4 Case studies</b>	<b>16</b>
25	4.1 Measurements . . . . .	16
26	4.2 Forecasts . . . . .	17
27	<b>5 Results</b>	<b>17</b>
28	5.1 Overall performance of the methods . . . . .	17
29	5.2 Detailed insight through the decomposition of the CRPS . . . . .	19
30	5.3 Detailed insight through the CRPS Moments-Contributions . . . . .	23
31	<b>6 Discussion</b>	<b>24</b>
32	6.1 Deterministic-based approach versus ensemble-based approach . . . . .	24
33	6.2 Discussion related to CRPS Moments-Contributions . . . . .	26
34	<b>7 Conclusions</b>	<b>30</b>
35	<b>Appendix A</b> Quality check	<b>33</b>
36	<b>Appendix B</b> standard deviation of EPS members distribution and observa-	
37	tions for the six sites	41
38	<b>Appendix C</b> of the optimal $\alpha$	<b>43</b>

## 39 1. Introduction

40 Operations of electrical power systems are becoming more challenging as the share of  
41 solar energy increases. In particular, due to the intrinsic variability of the solar resource,  
42 high penetration of solar power generation into the electrical grid may put in danger the  
43 grid supply-demand balance. Energy storage systems (EES) are one of the means used to  
44 ensure the grid stability. Notwithstanding, accurate PV power forecasting is a cost-effective  
45 way to size and operate ESS optimally. Consequently, PV power forecasts facilitate the  
46 large-scale integration of solar energy into the grid. In addition, for energy trading, accurate  
47 PV power forecasts are also required because penalties in proportion with the forecast errors  
48 are applied.

49 In this study, however, we focus on the global horizontal solar irradiance (GHI) forecasts  
50 instead of PV power forecasts. The present work constitutes thus a first step in assessing  
51 the contribution of the proposed methodologies for improving the quality of the PV power  
52 forecasts and of their potential gain for improved grid operations. Day-ahead GHI forecasts  
53 are treated here as they have been considered essential to secure the power grid [1]. More-  
54 over, we propose to work on probabilistic forecasting in order to estimate the uncertainty  
55 associated to day-ahead GHI forecasts. This additional knowledge permits for instance grid  
56 operators to improve their decisions regarding the grid operations. The interested reader can  
57 refer to [2] or [3] to understand the benefits of a probabilistic forecast against a deterministic  
58 one.

59 Day-ahead GHI forecasts are classically generated by Numerical Weather Predictions  
60 models (NWP). For instance, The Integrated Forecasting System (IFS) model of the Eu-  
61 ropean Centre of Medium-Range Weather Forecasts (ECMWF) provides day-ahead GHI  
62 forecasts [4]. The forecasts can take either the form of a deterministic forecast or an en-  
63 semble forecast denoted by the term Ensemble Prediction System (EPS). EPS consists in  
64 a set of several perturbed forecasts of irradiance, each representing a possible future state  
65 of the atmosphere. If an EPS gives an important information about the uncertainty associ-  
66 ated to a forecast, it requires a high computational cost. Thus, the added value of EPS for  
67 probabilistic forecasting needs to be determined to justify their computation.

68 We propose below to conduct a bibliographic survey related to day-ahead solar forecasts  
69 with a special emphasis on the use of NWP outputs to generate probabilistic forecasts.  
70 One of the first approach used to generate day-ahead probabilistic irradiance forecasts was  
71 proposed by Lorenz et al. [5]. In this work, a Gaussian distribution of the error of the  
72 ECMWF-IFS deterministic irradiance forecast was used to generate prediction intervals.  
73 Alessandrini et al. [6] developed an analog statistical method approach applied to a set of  
74 explanatory weather variables (GHI, cloud cover, air temperature, etc.) provided by the  
75 NWP Regional Atmospheric Modeling System (RAMS) to generate probabilistic PV power  
76 forecasts for three solar farms located in Italy. Zamo et al. [7] proposed two statistical  
77 approaches to generating probabilistic forecasts of daily PV production from information  
78 provided by Météo France's EPS, PEARP. The first approach makes use of the PEARP  
79 control member as unique input to quantile regression methods while the second one averages  
80 the set of quantiles calculated from each of the 35 members of the PEARP ensemble. Bacher

81 et al. [8] used a weighted quantile regression (WQR) technique to compute up to 24h ahead  
82 probabilistic PV forecasts. In addition to lagged PV measurements, the WQR model used  
83 also a NWP-based GHI deterministic forecast. Lauret et al. [9] used the IFS model to  
84 produce quantile forecasts of solar irradiance and Iversen et al. [10] introduces the idea of  
85 modeling uncertainty by stochastic differential equations from a NWP-based deterministic  
86 forecast provided by the Danish Meteorological Institute. Bakker et al. [11] proposed a  
87 comparison of seven statistical regression models to issue GHI probabilistic forecasts from  
88 the deterministic numerical weather prediction (NWP) model HARMONIE-AROME (HA)  
89 and the atmospheric composition model CAMS.

90 It must be noted that the above cited works make use of deterministic information  
91 extracted from NWP models to generate probabilistic forecasts with the help of statistical  
92 techniques like quantile regression or analog ensemble. Others authors like Sperati et al.  
93 [12] proceeded differently. In their work, Sperati et al. [12] generated up to 72h probabilistic  
94 forecasts from the raw EPS provided by the ECMWF. In this study, two post-processing  
95 methods (also called calibration techniques) applied to the initial raw ensemble were used  
96 to further improve the quality of the probabilistic forecasts. Massidda and Marrocu [13]  
97 went a little bit further and proposed a methodology to combine ECMWF ensemble and the  
98 high-resolution IFS deterministic forecast.

99 If we extend our bibliographic survey to the probabilistic predictions of other weather  
100 variables such as wind, temperature or precipitation, more publications can be found on  
101 how to use information from NWP models to generate probabilistic forecasts. For example,  
102 Pinson [14] and Pinson and Madsen [15] suggested a framework for the calibration of wind  
103 ensemble forecasts. Junk et al. [16] proposed an original calibration model for wind-speed  
104 forecasting applied to ECMWF-EPS based on the combination between Nonhomogeneous  
105 Gaussian Regression and Analog Ensemble Models. Likewise, Hamill and Whitaker [17]  
106 suggested an adaptation of the analog ensemble technique for the calibration of ensemble  
107 precipitation forecast, using the statistical moments of the distribution such as mean and  
108 spread of the members as predictors.

109 Wilks [18], followed in his methodology by Williams et al. [19], compared several post-  
110 processing techniques of weather EPS forecasts, such as ensemble dressing, Logistic Re-  
111 gression, Nonhomogeneous Gaussian Regression (NGR) and Rank-Histogram recalibration.  
112 The reader can refer to [20] and [21] for more details regarding the parametric calibration  
113 of ensemble forecasts with techniques like NGR with a special emphasis on the choice of the  
114 type of the parametric distribution used by the regression technique. Finally, the interested  
115 reader should consult the reference book [24], which proposes a summary of the common  
116 probabilistic forecasting ensemble-based models with their respective pros and cons.

117 Based on this bibliographic survey, two different approaches for day-ahead GHI proba-  
118 bilistic forecasting with the help of NWP models can be identified, which we denoted here  
119 by approaches 1 and 2 :

- 120 1. Approach 1 referred herein as *deterministic-based models* : the probabilistic forecast  
121 is computed from deterministic NWP predictors with the help of statistical methods.  
122 Linear Quantile Regression and Analog Ensemble techniques are particularly attractive

123 to implement this methodology.

- 124 2. Approach 2 referred herein as *ensemble-based models* : the estimation of the forecast  
 125 is made through the calibration of an EPS or from information (for example mean or  
 126 spread) inferred from the ensemble. For instance, calibration techniques like Nonho-  
 127 mogeneous Regression can be used to improve the raw ensemble EPS. Also, methods  
 128 based on Linear Quantile Regression and Analog methods can be used to produce  
 129 probabilistic forecasts from the mean and spread of the ensemble.

130 It must be stressed however that, to the best of our knowledge, no previous works have  
 131 been dedicated to the comparison of the two approaches and particularly in the realm of  
 132 solar probabilistic forecasts. In this work, our main goal is therefore to assess the relative  
 133 merits of each approach for day-ahead GHI probabilistic forecasts. Besides, we would like  
 134 to highlight the possible added-value brought by EPS for probabilistic forecasting. Indeed,  
 135 it is well known that the generation of such ensemble necessitates high computing capacities  
 136 compared to a single deterministic forecast that is fed into a statistical method to produce  
 137 the probabilistic forecasts. More precisely, it should be noted that the calculation cost is  
 138 not the same to produce only the control member of EPS or the whole set of members.

139 To understand the benefits associated with the usage of EPS, we propose in this paper a  
 140 sound and consistent methodology to evaluate the respective contribution of each approach.  
 141 First, the quality appraisal of the different models will be made according the verification  
 142 framework proposed by Lauret et al. [25]. This framework (which is not consistently pro-  
 143 posed in the literature) is based on visual diagnostic tools and numerical scores like the  
 144 Continuous ranked Probability Score (CRPS) which permits to objectively rank the com-  
 145 peting forecasting methods. However, this classical verification framework is not sufficient to  
 146 completely explain the contribution of the statistical moments of the forecast distributions  
 147 to the forecast quality. That is why we propose in a second step a new tool that evaluates  
 148 the accuracy of all moments of the forecast distribution and its contribution to the CRPS  
 149 score. We hope that this new diagnostic tool will provide a more in-depth understanding  
 150 of the performance of each approach. To this end, we evaluate models that generate day-  
 151 ahead GHI probabilistic forecasts on 6 sites that experience different sky conditions. The  
 152 probabilistic models are built :

- 153 1. With only the control member of the EPS as a deterministic predictor (deterministic-  
 154 based approach),  
 155 2. With a deterministic predictor inferred from the whole set of EPS's members. The  
 156 first statistical moment (mean of the members) can be such a deterministic predictor  
 157 (ensemble-based approach),  
 158 3. With several predictors inferred from the ensemble like the mean and the variance of  
 159 the ensemble (ensemble-based approach).

160 We propose the following structure for the paper. Section 2 introduces the different  
 161 forecasting models while section 3 briefly presents the diagnostic tools used for the verifica-  
 162 tion of probabilistic forecasts. Section 4 presents the case studies and details the data used  
 163 to evaluate the different probabilistic models. Section 5 provides a detailed assessment of



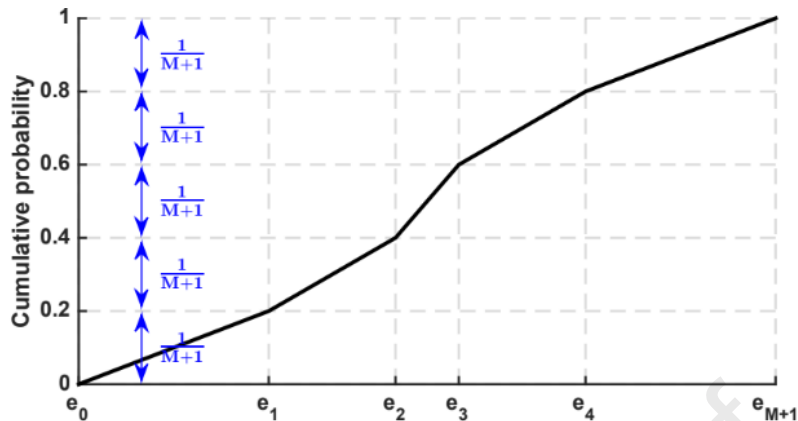


Figure 1: Illustration of an uniform construction of a CDF from an ensemble of  $M = 4$  members ( $e_1, e_2, e_3, e_4$ ). The tails of the CDF are bounded by  $e_0$  and  $e_{M+1}$  which correspond to the minimum and the maximum of the climatology.

164 the performance of the different methods. Finally, a discussion will be conducted in sec-  
 165 tion 6, trying to understand the pros and cons of each forecasting methods and the factors  
 166 impacting the forecast quality.

## 167 2. Building probabilistic forecasts

168 Regarding probabilistic forecasts of continuous predictand like GHI, a probability state-  
 169 ment i.e. either a Probability Distribution Function (PDF)  $f$  or a Cumulative Distribu-  
 170 tion Function (CDF)  $F$  encodes the uncertainty of the forecast. In this work, three ways to  
 171 estimate this CDF or PDF are considered: parametric PDFs, discrete quantile estimates of  
 172 a CDF via a non-parametric method and CDF derived from EPS.

173 In this study, the EPS is provided by the European Centre of Medium-Range Weather  
 174 Forecasts (ECMWF). It corresponds to 50 perturbed members and a control run (unper-  
 175 turbed member) [4] that give the cumul of the GHI with a 3 hours time step. This leads  
 176 to a total of  $M = 51$  members. An EPS can be seen as discrete estimates of a CDF when  
 177 they are sorted in ascending order. Lauret et al. [25] discussed three ways to associate these  
 178 sorted members to cumulative probabilities. In this work, we chose the uniform distribution  
 179 which consists in a uniform spacing of the members and a linear interpolation between the  
 180 members. More precisely, this choice assigns a probability mass of  $1/(M + 1)$  between two  
 181 members and for events that fall outside of the ensemble. Using this definition, the  $i^{th}$   
 182 ensemble member can be interpreted as a quantile forecast with a probability level equal  
 183 to  $\tau = \frac{i}{M+1}$ . Put differently, the ECMWF ensemble forecasts are in the form of 51 equally  
 184 spaced quantiles with probability levels  $\tau = \frac{1}{52}, \frac{2}{52}, \dots, \frac{51}{52}$ . This construction is illustrated  
 185 in Figure 1, for an EPS with 4 members. In the following, we present first the different  
 186 statistical techniques used to estimate the uncertainty of the forecasts. Secondly, we detail  
 187 the two approaches introduced in section 1.

188 2.1. Statistical techniques used to generate probabilistic forecasts

189 2.1.1. The linear quantile regression (LQR) technique

This method estimates the quantiles of the cumulative distribution function  $F$  of some response variable  $Y$  (also called predictand) by assuming a linear relationship between the quantiles of  $Y$ , namely  $q_\tau$  and a set of explanatory variables  $X$  (called predictors):

$$q_\tau = \beta_\tau X + \epsilon, \quad (1)$$

190 where  $\beta_\tau$  is a vector of parameters to optimize for each probability level  $\tau$  and  $\epsilon$  represents  
191 a random error term.

192 Following Koenker [26], the

vector  $\hat{\beta}_\tau$  that defines each quantile is obtained as the solution of the following minimization problem:

$$\hat{\beta}_\tau = \arg \min_{\beta} \sum_{i=1}^N \Psi_\tau (Y_i - \beta X_i). \quad (2)$$

193 where  $N$  is the number of pairs of observed predictand  $Y_i$ , set of predictors  $X_i$  taken from  
194 the training set.  $\Psi_\tau(u)$  is the quantile loss function defined as :

$$\Psi_\tau(u) = \begin{cases} u\tau & \text{if } u \geq 0, \\ u(\tau - 1) & \text{if } u < 0, \end{cases} \quad (3)$$

195 with  $\tau$  representing the quantile probability level. Hence, in quantile regression, the quantiles  
196 are estimated by applying asymmetric weights to the mean absolute error.

197 Thus, the quantity  $\hat{q}_\tau = \hat{\beta}_\tau X$  is the estimation of the  $\tau^{th}$  quantile obtained by the LQR  
198 method.

199 It must be noted that the quantile regression method estimates each quantile separately  
200 (i.e. the minimization of the quantile loss function is made for each  $\tau$  separately). As a  
201 consequence, one can obtain quantile regression curves that may intersect, i.e  $\hat{q}_{\tau_1} > \hat{q}_{\tau_2}$   
202 when  $\tau_1 < \tau_2$ . To avoid this issue during the model fitting, we used the rearrangement  
203 method described by Chernozhukov et al. [27].

204 Figure 2 shows some quantiles estimates of the CDF of the predictand  $Y$  (here GHI)  
205 as a function of the day-ahead forecasted GHI. Hence, in this case, the predictor  $X$  is the  
206 predicted irradiance which will be represented in this work either by the ECMWF control  
207 member or the mean of the ECMWF ensemble (see Table 2 below). This example shows that  
208 the forecast uncertainty depends on the level of the predicted irradiance. More precisely,  
209 and as shown by Figure 2, the dispersion of points is lower for values of predicted irradiance  
210 close to  $0 \text{ W/m}^2$  and greater for values between  $40$  and  $100 \text{ W/m}^2$ .

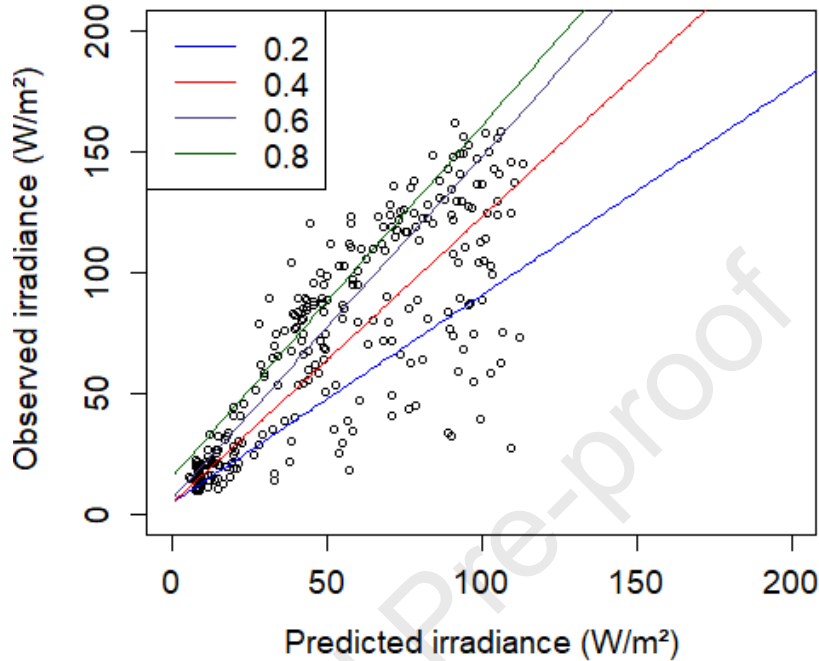


Figure 2: Observed GHI vs. the predicted day-ahead GHI. The lines are the estimates of the quantiles with probability levels of 0.2, 0.4, 0.6 and 0.8. Data are from the training period of Hawaii. Observed and predicted GHI are averaged on the 3-hour window [17h-20h] local time.

### 2.1.2. The Analog Ensemble (AnEn) technique

The analog ensemble technique is now quite a standard in the energy meteorology forecasting community [29, 17]. Similarly to the LQR method, the analog technique is a non-parametric method that can be used to estimate the predictive CDF of the predictand.

Considering a training set of  $N$  ordered (sorted by forecasts) pairs of GHI observations/GHI forecasts  $(Y_i, \hat{Y}_i)_{i=1, \dots, N}$ , the procedure for determining the forecast CDF is as follows:

1. For a new forecast taken from a testing set, calculate its distance from every past forecast order and find the rank  $R$  of the past forecast that is the closest to the new forecast.
2. Form an ensemble by selecting the  $2\alpha + 1$  past training observations  $Y_k$  having their ranks  $k$  inside the interval  $[R - \alpha, R + \alpha]$ .
3. Compute the predictive CDF at a specific value  $y$  of the predictand using the following equation:

$$\hat{F}(y) = P(Y \leq y) = \frac{1}{2\alpha + 1} \sum_{k=1}^{2\alpha+1} H(y - Y_k), \quad (4)$$

223 where  $Y$  is the random value related to the predictand (here GHI) and  $H$  is the Heaviside  
 224 or step function. The effectiveness of the method is strongly dependent on the value of  $\alpha$ .  
 225 It is proposed here to take  $\alpha = 0.02N$ . This choice has been motivated by a preliminary  
 226 study made on the training period. Appendix C details the selection of the optimal value  
 227 of  $\alpha$ . Finally, as for the linear quantile regression, note that the GHI forecasts used in the  
 228 *AnEn* technique will be given either by the ECMWF control member or the mean of the  
 229 ensemble (see Table 2 below).

### 230 2.1.3. The Nonhomogeneous truncated Gaussian Regression technique ( $t\_NGR$ )

The NGR technique also called in some studies “Ensemble Model Output Statistics” (EMOS) has been introduced by Gneiting et al. [20] for probabilistic forecasting of weather variables. This technique is dedicated to the post-processing of ensemble forecasts produced by an EPS. The NGR technique builds the predictive PDF of the predictand  $Y$  from a normal PDF. As such, this kind of model can be termed as a parametric model. The predictive pdf  $\hat{f}$  estimated by the NGR method is given by:

$$\hat{f} \sim \mathcal{N}\left(a + \sum_{k=1}^M (b_k m_k), c + dS^2\right), \quad (5)$$

231 where  $M$  is the number of members,  $m_k$  is the  $k^{th}$  member and  $S^2$  is the variance of the  
 232 ensemble members distribution. The free parameters  $a, b_1, \dots, b_M, c$  and  $d$  are determined  
 233 with the help of an optimization procedure. In this work, and following Gneiting et al.  
 234 [20], these parameters are calculated by minimizing (over a training period) an evaluation  
 235 metric for probabilistic forecasts called CRPS (see section 3.2 for details regarding CRPS).  
 236 Furthermore, as GHI is a necessarily positive quantity, we propose, in this work, a variant  
 237 of the NGR technique namely a truncated version (at 0) of the nonhomogeneous gaussian  
 238 regression. In the following, the corresponding model is denoted as  $t\_NGR$ .

### 239 2.1.4. The Nonhomogeneous Regression of Generalized Extreme Value technique ( $NR\_GEV$ )

240 One can question the choice of a Gaussian distribution in the  $t\_NGR$  technique. Indeed,  
 241 the distributions of observations for a fixed forecasting level are actually non-Gaussian. Two  
 242 examples for the studied sites are presented in Figure 3.

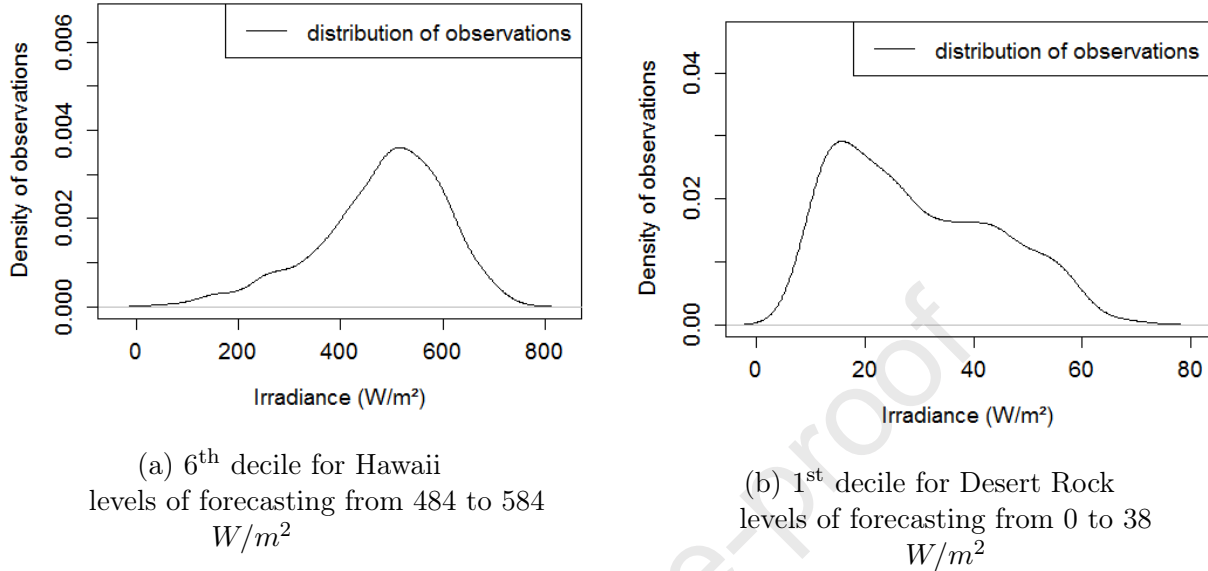


Figure 3: Example of distributions of observations for a fixed forecasting level.

243 On these specific examples, the distributions of observations are clearly non-Gaussian  
244 and the consideration of other types of distributions may improve the skills of the forecast.

245 As pointed out in [21] and [22], other types of parametric distributions can be used  
246 to deal with this issue. Here, a Non homogeneous Regression approach with Generalized  
247 Extreme Value distributions is proposed to estimate the PDF of the predictand  $Y$ . The  
248 PDF of a generalized Extreme value distribution for a specific value  $y$  of the predictand  
249 GHI is defined as :

$$\hat{f}(y) = \begin{cases} \frac{1}{\sigma} \left[ 1 + \xi \left( \frac{y-\mu}{\sigma} \right) \right]^{(-\frac{1}{\xi})-1} \exp \left( - \left[ 1 + \xi \left( \frac{y-\mu}{\sigma} \right) \right]^{-\frac{1}{\xi}} \right) & \xi \neq 0, \\ \frac{1}{\sigma} \exp \left( -\frac{y-\mu}{\sigma} \right) \exp \left[ - \exp \left( -\frac{y-\mu}{\sigma} \right) \right] & \xi = 0. \end{cases} \quad (6)$$

250 The parameters  $\mu$ ,  $\sigma$  and  $\xi$  are to be determined by optimizing the CRPS over the  
251 training period. We followed the framework of [31] and [32] to set these coefficients. Fol-  
252 lowing this procedure, the mean  $\mu$  and the scale parameter  $\sigma$  of the final distributions are  
253 determined by linear regression, and depends only on variables inferred from the EPS. The  
254 mean is a linear combination of the mean of the members and the fraction of members  
255 which predict exactly zero. The scale parameter  $\sigma$  depends on the ‘‘Gini’s mean difference’’  
256 (a measure of the variability closely related to the spread of the members, see [33] for de-  
257 tails). Note that the shape parameter is taken as a constant. Thus, the minimization of the  
258 CRPS yields the linear coefficients for the mean  $\mu$  and the scale parameter  $\sigma$  as well as the  
259 value of the shape parameter  $\xi$ . Note that the two techniques namely  $t\_NGR$  discussed

Site	HAW	DR	SP	PAL	TIR	LAN
Any perturbed member	138	75.3	126.5	97.7	110.7	98.8
Control member	135	72.8	91.9	102.9	100.8	93.2
Mean of the members	129.7	67.9	113.8	81.8	92.6	84.3
Median of the members	133.9	69.4	115.5	84.1	94.7	85.6

Table 1: RMSE ( $W/m^2$ ) of 4 deterministic forecasts that can be inferred from an EPS: any of the 50 perturbed members of ECMWF ensemble forecast, the control member (unperturbed), the mean of the members and the median of the members. See Table 3 for the signification of the acronyms of the different sites.

260 above and  $NR\_GEV$  discussed here are part of a family of parametric methods named  
 261 Nonhomogeneous Regression ( $NR$ ).

### 262 2.2. Obtaining probabilistic forecasts from deterministic forecasts (Deterministic-based ap- 263 proach)

264 Some of the techniques presented in section 2.1, namely the Linear Quantile Regression  
 265 (LQR) and the Analog Ensemble (AnEn) techniques, are capable of generating a probabilistic  
 266 forecast from a deterministic predictor.

267 In our study, and regarding the deterministic-based approach, the control member of  
 268 ECMWF-EPS is the predictor variable  $X$  of the LQR technique and it will be the forecast  
 269 used in the AnEn procedure. The corresponding probabilistic models are denoted respec-  
 270 tively as  $LQR_c$  and  $AnEn_c$  in the following.

### 271 2.3. Obtaining probabilistic forecasts from ensemble forecasts (Ensemble-based approach)

#### 272 2.3.1. From the raw output of ECMWF-EPS

273 Given a raw ensemble forecast of  $M$  members  $\{m_i\}_{i=1,\dots,M}$ , it seems natural to define  
 274 directly a forecast CDF from this EPS as illustrated in Figure 1. Note that this definition  
 275 corresponds to the “uniform” definition of a CDF derived from an ensemble” discussed in  
 276 Lauret et al. [25].

#### 277 2.3.2. From information extracted from an EPS

278 An EPS differs from a deterministic forecast by the multiplicity of predictors. In this  
 279 work, we propose to assess the quality of two variants of probabilistic models built with  
 280 information extracted from an EPS.

281 The first variant will make use of the mean of the ensemble members of the EPS. The  
 282 use of the mean of members as a deterministic predictor is justified by Table 1. For all the  
 283 considered sites depicted in Table 3, Table 1 lists the Root Mean Square Error (RMSE)<sup>1</sup> of  
 284 different deterministic predictors extracted from an EPS.

285 As shown by Table 1, the mean of all the members turns out to be the best predictor for  
 286 deterministic forecasting. Hence, to quantify the improvement brought by the first moment

<sup>1</sup>RMSE is a common metric used to assess the accuracy of deterministic forecasts [34]

Approach	Deterministic-based		Ensemble-based			
Predictors	Control member		Mean of members		Mean and spread of members	
Technique	AnEn	LQR	AnEn	LQR	LQR	NR
Model Abbreviation	$AnEn_c$	$LQR_c$	$AnEn_m$	$LQR_m$	$LQR_s$	$t\_NGR$   $NR\_GEV$

Table 2: Summary of all considered forecasting models with AnEn: Analog Ensemble, LQR: Linear Quantile Regression, NR: Nonhomogeneous Regression

estimation (i.e. the mean), two models denoted by  $LQR_m$  and  $AnEn_m$  based respectively on the LQR and AnEn techniques will be evaluated.

The second variant will include, in addition to the mean of the members, the spread (i.e. the variance) of the members of the EPS. The  $t\_NGR$  and the  $NR\_GEV$  models described in sections 2.1.3 and 2.1.4 use the first and second moment of the EPS distribution to build the predictive distributions. Furthermore, we also propose to use the LQR technique with a vector  $X$  of predictors given by

$$X = [\mu, S^2], \quad (7)$$

where  $\mu$  represents the mean of members and  $S^2$  the variance of the ensemble. This method will be referred in this study as  $LQR_s$ . Finally, Table 2 summarizes the different probabilistic models that will be evaluated in this study.

### 3. Verification of the probabilistic forecasts

In this section, we detail some of the verification tools proposed by Lauret et al. [25] that will be applied to assess the quality of GHI probabilistic forecasts. Following this work, we will rely on a quantitative score namely the continuous ranked probability score (CRPS) and its related skill score (CRPSS) to rank objectively the different methods. Moreover, and based on the recommendations of [25], we will provide the decomposition of the CRPS into the main attributes that affect the quality of the forecasts. In addition to this decomposition, it is worth noting that we will propose in this work a new way to have detailed insight into the performance of the methods. This new methodology is based on the contribution of the moments (mean, variance, etc.) of the forecast distribution to the CRPS (see section 3.3 below).

#### 3.1. Attributes for a skillful probabilistic model

We recall here briefly the two main attributes that characterize the quality of the probabilistic models namely reliability and resolution [35, 36]. Reliability or calibration evaluates the statistical consistency between the forecasts and the observations. In the case of a continuous variable like GHI, a high reliability is obtained if predictive distributions and distributions of observations agree. Resolution refers to the ability of the probabilistic model to discriminate among different forecast situations. More precisely, the more distinct the observed frequency distributions for various forecast situations are from the full climatological distribution, the more resolution the forecast model has. A high quality probabilistic

317 model should issue reliable forecasts with high resolution. In other words, high reliability is  
 318 a necessary but not a sufficient condition for a high quality probabilistic forecast. The fore-  
 319 cast should also exhibit high resolution. For instance, climatological forecasts are perfectly  
 320 reliable but exhibit no resolution.

### 321 3.2. CRPS

322 In the verification framework proposed by Lauret et al. [25], the authors recommend the  
 323 computation of a score like the Continuous Ranked Probability Score (CRPS) to evaluate  
 324 the overall quality of the probabilistic models. We recall here the definition of the CRPS.

#### 325 3.2.1. Definition

The CRPS measures the difference between the predicted and observed cumulative dis-  
 tributions functions (CDF) [38]. The CRPS reads as

$$CRPS = \frac{1}{N} \sum_{i=1}^N \int_{-\infty}^{+\infty} \left[ \hat{F}_{fcst}^i(y) - F_{y_{obs}}^i(y) \right]^2 dy, \quad (8)$$

326 where  $\hat{F}_{fcst}(y)$  is the predictive CDF of the predictand  $Y$  (here GHI) and  $F_{y_{obs}}(y)$  is a  
 327 cumulative-probability step function that jumps from 0 to 1 at the point where the value  
 328 of the predictand  $y$  equals the observation  $y_{obs}$  (i.e.  $F_{y_{obs}}(y) = 1_{\{y \geq y_{obs}\}}$ ). The squared  
 329 difference between the two CDFs is averaged over the  $N$  forecast/observation pairs. The  
 330 CRPS score rewards concentration of probability around the step function located at the  
 331 observed value [35]. In other words, the CRPS penalizes lack of resolution of the predictive  
 332 distributions as well as biased forecasts. Note that the CRPS is negatively oriented (smaller  
 333 values are better) and it has the same dimension as the forecasted variable. CRPS is a  
 334 proper score meaning that it obtains the best expected value when the forecast distribution  
 335 is equal to the true distribution of probability of the observation. Besides, using proper  
 336 scoring rules allows the decomposition of the score into the two important attributes of the  
 337 quality of a forecasting probabilistic model namely resolution and reliability. This permits  
 338 to understand more precisely the characteristics of the quality of the forecast.

#### 339 3.2.2. CRPS Skill Score

340 In a similar manner, skill scores are used to assess the forecast skill of deterministic  
 341 forecasts [39], Pedro et al. [40] used the CRPS Skill Score (CRPSS) to gauge the quality of  
 342 their probabilistic forecasting models against a reference method. The CRPSS metric (in  
 343 %) reads as

$$CRPSS = 100 \times \left( 1 - \frac{CRPS_m}{CRPS_r} \right), \quad (9)$$

344 where  $CRPS_r$  denotes the CRPS of the reference method and  $CRPS_m$  refers to the CRPS  
 345 of the model under evaluation (see Table 2). A negative value of CRPSS indicates that  
 346 the probabilistic method fails to outperform the reference model while a positive value of



347 CRPSS means that the forecasting method improves on the reference model. Further, the  
 348 higher the CRPSS, the better the improvement.

349 In this work, and following the recommendations of Doubleday et al. [41], the raw output  
 350 of the ECMWF-EPS serves as the reference benchmark model.

### 351 3.2.3. Decomposition of the CRPS

The decomposition of the CRPS is given by :

$$CRPS = REL - RES + UNC, \quad (10)$$

352 where REL, RES and UNC are respectively the reliability part, the resolution part and the  
 353 uncertainty part of the CRPS. The interested reader is referred to [25] for details regarding  
 354 the computation of the different components of the CRPS.

355 In addition to reliability and resolution, the uncertainty term accounts for the variability  
 356 of the observations. It is an indication of the difficulty to forecast the variable of interest and  
 357 cannot be modified by the forecasting model. It is also worth noting that the uncertainty part  
 358 UNC corresponds to the score of the climatology. For scores like CRPS that are negatively  
 359 oriented, the goal of a forecasting model is to minimize (resp. maximize) as much as possible  
 360 the reliability term (resp. the resolution term). In fact, a forecasting model with a high  
 361 resolution term means that the model has captured the maximum of the variability present  
 362 in the data (which variability is measured by the uncertainty term).

### 363 3.3. Contributions of the statistical moments of the forecast distribution to the CRPS

364 In this study, a new methodology for a better understanding of the skills of a probabilistic  
 365 forecast in relation with the CRPS score is developed. The main idea is to assess separately  
 366 the contribution of the statistical moments (mean, variance, etc.) of the predictive distribu-  
 367 tions to the CRPS and consequently to the quality of a probabilistic forecasting model. The  
 368 principle of the method is to create two virtual forecasts which show the contribution of the  
 369 statistical moments of the actual forecast to the CRPS. Let us illustrate the methodology  
 370 with 3 forecast PDFs depicted in Figure 4.  $f$  represents the actual forecast PDF and  $f_{m1}$   
 371 and  $f_{m2}$  the associated virtual PDF forecasts.

The first virtual forecast  $f_{m1}$  is derived from the first moment (mean) of the actual  
 forecast  $f$ . Let  $m_1$  be the first moment of  $f$  and  $\delta$  the Dirac distribution (corresponding to  
 the dotted vertical line in Figure 4), the PDF of  $f_{m1}$  is thereby defined by:

$$f_{m1}(y) \equiv \delta(y - m_1). \quad (11)$$

372 Note that this definition implies that the second, third and further moments of  $f_{m1}$  are equal  
 373 to 0.

The second virtual forecast  $f_{m2}$  is given by a Gaussian distribution with first and second  
 moments equal to those of  $f$ . Let  $m_2$  be the second moment of  $f$ ,  $f_{m2}$  is defined as:

$$f_{m2} \sim \mathcal{N}(m1, m2). \quad (12)$$

374 Being a Gaussian distribution, the third, fourth and further moments of  $f_{m2}$  are equal to 0.

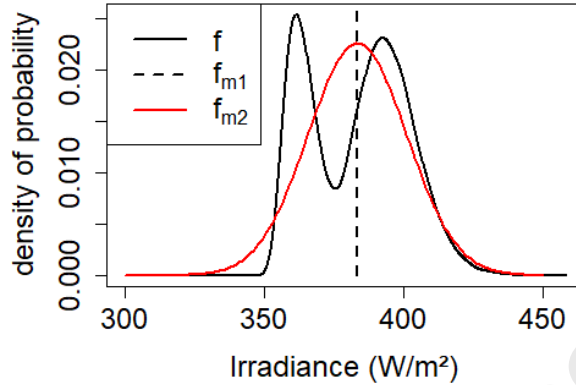


Figure 4: Illustration of the virtual forecasts  $f_{m1}$  and  $f_{m2}$  related to the forecast PDF  $f$

The contribution of the statistical moments of the distribution to the CRPS is computed as follows. First, the CRPS of each forecast namely  $CRPS_f$ ,  $CRPS_{f_{m1}}$  and  $CRPS_{f_{m2}}$  are averaged over the  $N$  forecast/observation pairs. This leads to the corresponding values  $CRPS$ ,  $CRPS_{m1}$  and  $CRPS_{m2}$ . Second, the difference  $G_2 = CRPS_{m1} - CRPS_{m2}$  and  $G_+ = CRPS_{m2} - CRPS$  are calculated. Note that one can therefore rewrite the CRPS as:

$$CRPS = CRPS_{m1} - G_2 - G_+. \quad (13)$$

375 Note that the  $CRPS_{m1}$  of the deterministic forecast  $f_{m1}$  is actually its Mean Absolute  
 376 Error (MAE)<sup>2</sup> (see [38] for details).

377  $G_2$  is the measure of the gain in CRPS or equivalently in forecast quality that results  
 378 from the additional information brought by the second moment of the distribution.  $G_+$   
 379 represents the gain resulting from the other statistical moments.  $G_2$  is assumed to be  
 380 positive. If it is found negative, then the probabilistic forecast has no added value compared  
 381 to a deterministic forecast. Indeed, the CRPS of the probabilistic forecast would be higher  
 382 than the CRPS of the deterministic one ( $CRPS_{m1}$ , which is the MAE), thus denoting a loss  
 383 of quality of the probabilistic forecast. On the other hand,  $G_+$  is generally positive. It can  
 384 be null or negative if the forecast distribution obtains a higher CRPS score than a Gaussian  
 385 distribution defined by  $\mathcal{N}(m1, m2)$ . This would indicate that the forecast distribution is less  
 386 suitable than a Gaussian distribution.

387 In section 5.3 below, we propose to present this diagnostic tool under the form of a bar-  
 388 plot, where  $CRPS$ ,  $G_+$  and  $G_2$  are stacked in this order.  $G_2$  is denoted by the pink part of  
 389 the bar,  $G_+$  by the green part and  $CRPS$  by the blue part. Note that a black line on the  
 390 top of the blue part is used to better highlight the value of the CRPS and a dotted black line

<sup>2</sup>Similarly to RMSE, MAE is also a common metric used to assess the accuracy of deterministic forecasts.

391 indicates  $CRPS_{m1}$  (see Figure 6). In the following, we refer to this diagnostic tool based on  
392 the contribution of the moments of the forecast distributions to the CRPS as “MC-CRPS”.

#### 393 4. Case studies

394 Six sites are chosen to test the selected models. The first one, Desert Rock, which is part  
395 of the SURFRAD network, is located in an arid area. It experiences a high occurrence of  
396 clear skies and consequently a very low variability. Two other sites, the airport of Hawaii,  
397 where the NREL set up a radiometric network, and Saint-Pierre, which is located on the  
398 coastal part of the island La Réunion, are insular sites. Both present a high yearly solar  
399 irradiation but also an important variability due to frequent partly cloudy skies. These  
400 differences between the two types of sites will permit testing the models under different sky  
401 conditions. For an extensive study on the multiple factors that impact the climatology and  
402 sky conditions in the specific case of Saint-Pierre and La Réunion, see Badosa et al. [42] or  
403 Kalecinski [43].

404 As the aforementioned sites exhibit a similar level of irradiation, three other BSRN sites  
405 namely Palaiseau, Tiruvallur and Langley are also considered to test our methodology. The  
406 six chosen sites experience different levels of annual solar irradiation and of sky conditions.  
407 Thus, this set of sites is representative of the various climates around the world. The main  
408 characteristics of these six sites are given in Table 3. The solar variability, presented in the  
409 last line of Table 3, is defined as the standard deviation of the changes in the clear sky index  
410 [44].

##### 411 4.1. Measurements

412 The measured data used in this work are global horizontal irradiance (GHI) time series  
413 recorded at the six considered sites. These datasets have been prepared for previous works  
414 related to the development and the benchmarking of probabilistic solar forecasts [45, 46].  
415 They correspond to two years of data divided in a training set (the first year) and test set  
416 (the second year). As the ensemble forecasts used here are provided with a 3-hour time step,  
417 the recorded time series, initially formatted with a 1-hour granularity, were averaged with  
418 a 3-hour time step. A quality check and several test were performed on the recorded GHI  
419 time series. The results are given in Appendix A.

	<b>Desert Rock (USA)</b>	<b>Hawaii (USA)</b>	<b>Saint-Pierre (Reunion)</b>
Acronym	DR	HAW	SP
Provider	SURFRAD	NREL	PIMENT
Position	36.6N, 119.0W	21.3N, 158.1W	21.3S, 55.5E
Elevation (m)	1007	11	75
Climate type	Desert	Insular tropic	Insular tropic
Years of record	2012 - 2013	2010-2011	2012 - 2013
Annual solar irradiation ( $MWh/m^2$ )	2.105	1.969	2.053
Solar variability 1-h ( $\sigma\Delta kt_{1hour}^*$ )	0.146	0.209	0.241
	<b>Palaiseau (France)</b>	<b>Tiruvallur (India)</b>	<b>Langley (USA)</b>
Acronym	PAL	TIR	LAN
Provider	BSRN	BSRN	BSRN
Position	48.7N, 2.2E	13.1N, 80.0E	37.1N, 76.4W.
Elevation (m)	156	36	3
Climate type	Mild oceanic	Monsoon	Humid
Years of record	2016-2017	2018-2019	2015-2016
Annual solar irradiation ( $MWh/m^2$ )	1.172	1.835	1.685
Solar variability 1-h ( $\sigma\Delta kt_{1hour}^*$ )	0.281	0.190	0.186

Table 3: Main characteristics of time series of recorded global horizontal irradiance (GHI) used to test the models.

#### 4.2. Forecasts

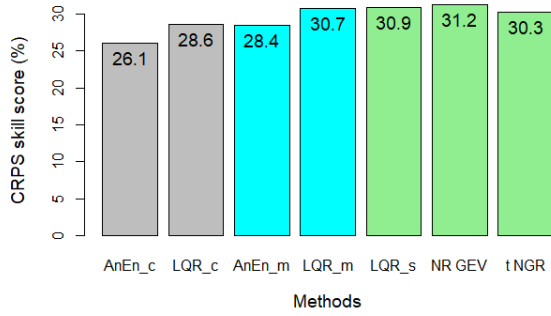
As mentioned above, the initial day-ahead ensemble forecasts, covering the same period as the measurements, are provided by the European Centre of Medium-Range Weather Forecasts (ECMWF). The EPS is released by ECMWF at 12:00 for the 72 next hours with a 3-hours timestep which allows it to be used for day-ahead scheduling or trading purposes.

## 5. Results

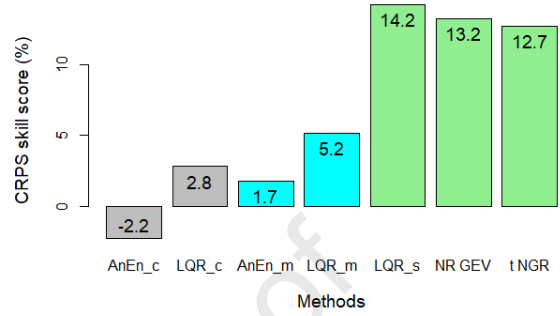
Based on the verification framework proposed by Lauret et al. [25], the overall performance of the different probabilistic methods is measured by the CRPS and the CRPSS. Detailed insight in the quality of the models is obtained through the decomposition of the CRPS and the new ‘‘MC-CRPS’’ method. Note that this section is dedicated to the presentation of the main results of the study. The next section will be devoted to an in-depth discussion related to the pros and cons of each approach and the added-value brought by the MC-CRPS methodology.

### 5.1. Overall performance of the methods

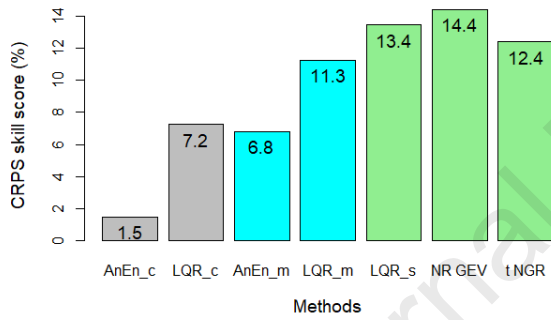
Table 4 lists the CRPS obtained by the different methods. However, in order to better highlight the relative merits of each approach, Figure 5 shows the CRPS skill scores of all



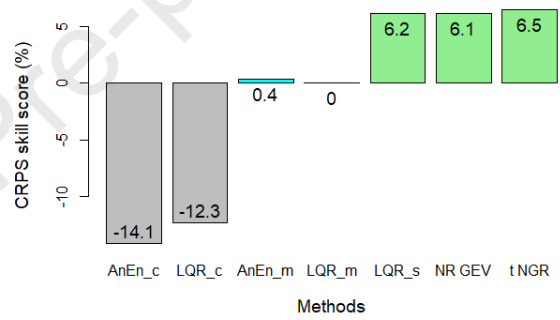
(a) Hawaii



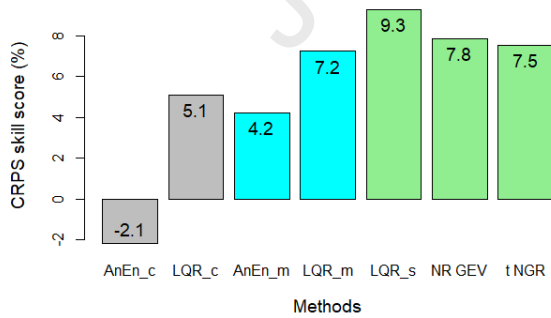
(b) Desert Rock



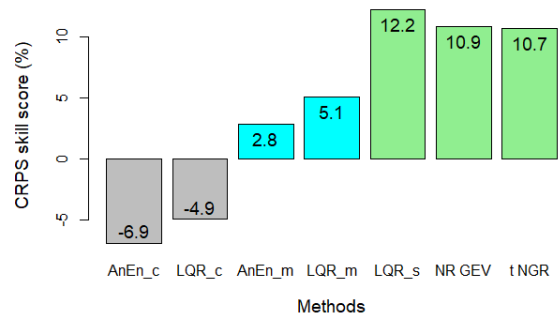
(c) Saint-Pierre



(d) Palaiseau



(e) Tiruvallur



(f) Langley

Figure 5: CRPS Skill Score of all models for the six considered sites. Grey : deterministic-based approach, Cyan : ensemble-based approach using the mean of the members, Green : ensemble-based approach using mean and standard deviation of the members.

436 the forecasting models. Let us recall that positive values of skill scores mean that the model  
 437 outperforms the reference model (here the raw ECMWF-EPS) while negative values reveal  
 438 that the quality of the evaluated model is worse than the reference one.

439 As shown by Figure 5, regardless the site under study, the highest CRPS skill scores are  
 440 obtained by the ensemble-based approach (represented by the cyan and green bars). Con-  
 441 versely, except the case of Hawaii, the deterministic-based approach (grey bars) yields lower  
 442 or even negative skill scores. These negative CRPS values indicate that the deterministic-  
 443 based models do not always achieve to increase the quality of the raw ensemble forecasts  
 444 (see for example Palaiseau and Langley).

445 A deeper look into the performance of the ensemble-based approach shows that models  
 446 using the mean and the standard deviation of the ensemble members (green bars) exhibit  
 447 a better forecast skill than models using only the mean of the members (cyan bars) albeit  
 448 the improvement is less pronounced for Hawaii. Overall, the model with the highest skill  
 449 score appears to be either  $LQR_s$  or  $NR\_GEV$ . Regarding the latter, it may suggest that  
 450 a judicious choice of the underlying PDF (see Equation 6) used by a calibration technique  
 451 like Nonhomogenous Regression (NR) can further improve the quality of the probabilistic  
 452 forecasts.

453 Finally, in order to quantify the relative improvement provided by the ensemble-based  
 454 approach over the deterministic-based approach, we calculate the gain in CRPS based on  
 455 the CRPS values of the best performer of each approach. It appears that the level of  
 456 improvement is very dependent on the studied site. It is moderate for Hawaii and Tiruvallur  
 457 (4%), becomes larger for Saint-Pierre (approximately 8%) and quite significant for Desert  
 458 Rock (approximately 12%), Langley and Palaiseau (approximately 16%).

## 459 5.2. Detailed insight through the decomposition of the CRPS

460 Table 4 also provides the decomposition of the CRPS into reliability and resolution of  
 461 the different forecasting methods. As mentioned previously, a forecast should exhibit a  
 462 small reliability term and a large resolution term. It is worth mentioning first that all  
 463 models significantly improves the reliability component of the raw EPS forecasts and that  
 464 the level of improvement strongly depends on the reliability of the initial raw ensemble.  
 465 Second, it can be noted that the reliability of all calibrated forecasts is fairly comparable.  
 466 In addition, regardless the site, it appears that, overall, the ensemble-based approach does  
 467 not significantly improve reliability compared to the deterministic-based approach. Looking  
 468 in more details, models based on the *AnEn* technique often appears to generate the most  
 469 reliable forecasts while the  $t\_NGR$  model generally provides the less reliable forecasts. Also,  
 470 in the case of Non homogeneous calibration technique, *GEV* distributions seem to be more  
 471 suitable than Gaussian distributions, since  $NR\_GEV$  is slightly more reliable than the  
 472  $t\_NGR$  model.

473 Regarding the resolution component, it must be noted first that the deterministic-based  
 474 approach fails to improve the resolution of the raw Ensemble. Conversely, resolution in-  
 475 creases with the ensemble-based approach, and particularly when the spread of EPS mem-  
 476 bers is taken as an input of the models i.e. case of the  $LQR_s, t\_NGR$  and  $NR\_GEV$

	Site	HAW	DR	SP	PAL	TIR	LAN
CRPS ( $W/m^2$ )	raw Ensemble	<b>67.7</b>	29.4	<b>59.4</b>	38.6	46.8	40.0
	<i>AnEn<sub>c</sub></i>	50.1	<b>30.1</b>	58.5	<b>44.0</b>	<b>47.8</b>	<b>42.8</b>
	<i>LQR<sub>c</sub></i>	48.4	28.6	55.1	43.3	44.4	42.0
	<i>AnEn<sub>m</sub></i>	48.5	28.9	55.3	38.4	44.9	38.9
	<i>LQR<sub>m</sub></i>	46.9	27.9	52.7	38.6	43.4	38.0
	<i>LQR<sub>s</sub></i>	46.8	<b>25.2</b>	51.4	<b>36.2</b>	<b>42.5</b>	<b>35.2</b>
	<i>t_NGR</i>	47.2	25.7	52.0	<b>36.2</b>	43.3	35.8
	<i>NR_GEV</i>	<b>46.6</b>	25.5	<b>50.8</b>	<b>36.2</b>	43.2	35.7
Reliability ( $W/m^2$ )	raw Ensemble	23.2	8.4	13.4	7.5	11.5	8.2
	<i>AnEn<sub>c</sub></i>	4.2	4.8	6.6	4.9	7.2	4.8
	<i>LQR<sub>c</sub></i>	4.4	5.3	7.1	5.4	6.7	5.3
	<i>AnEn<sub>m</sub></i>	4.1	4.7	6.2	4.9	7.9	4.5
	<i>LQR<sub>m</sub></i>	4.4	5.7	7.0	5.7	8.2	5.0
	<i>LQR<sub>s</sub></i>	4.5	5.9	7.6	5.3	8.2	5.4
	<i>t_NGR</i>	4.7	6.5	8.4	5.4	8.0	5.7
	<i>NR_GEV</i>	4.1	6.2	7.2	5.4	7.8	5.8
Resolution ( $W/m^2$ )	raw Ensemble	113.3	154.0	126.7	95.4	125.7	122.5
	<i>AnEn<sub>c</sub></i>	111.9	149.7	120.8	87.4	120.4	116.4
	<i>LQR<sub>c</sub></i>	113.9	151.7	124.7	88.6	123.3	117.7
	<i>AnEn<sub>m</sub></i>	113.4	150.8	123.5	93.0	124.0	120.0
	<i>LQR<sub>m</sub></i>	115.3	152.8	127.0	93.6	125.8	121.4
	<i>LQR<sub>s</sub></i>	115.5	155.6	128.9	95.6	126.8	124.7
	<i>t_NGR</i>	115.3	155.7	129.0	95.8	125.8	124.3
	<i>NR_GEV</i>	115.3	155.6	129.1	95.6	125.7	124.5
Uncertainty ( $W/m^2$ )	All Models	157.8	175.0	172.7	126.5	161.0	154.4

Table 4: CRPS and its components reliability, resolution and uncertainty of all considered models for the 6 sites. Cyan : deterministic-based approach, Green : ensemble-based approach. Red values indicate the worst CRPSs while the black bold ones show the best CRPSs.

477 models. Finally, one can state that the decomposition of the CRPS given in Table 4 re-  
 478 veals that the difference in quality between the two approaches is mainly explained by the  
 479 resolution component, whereas reliability is fairly comparable.

### 480 5.3. Detailed insight through the CRPS Moments-Contributions

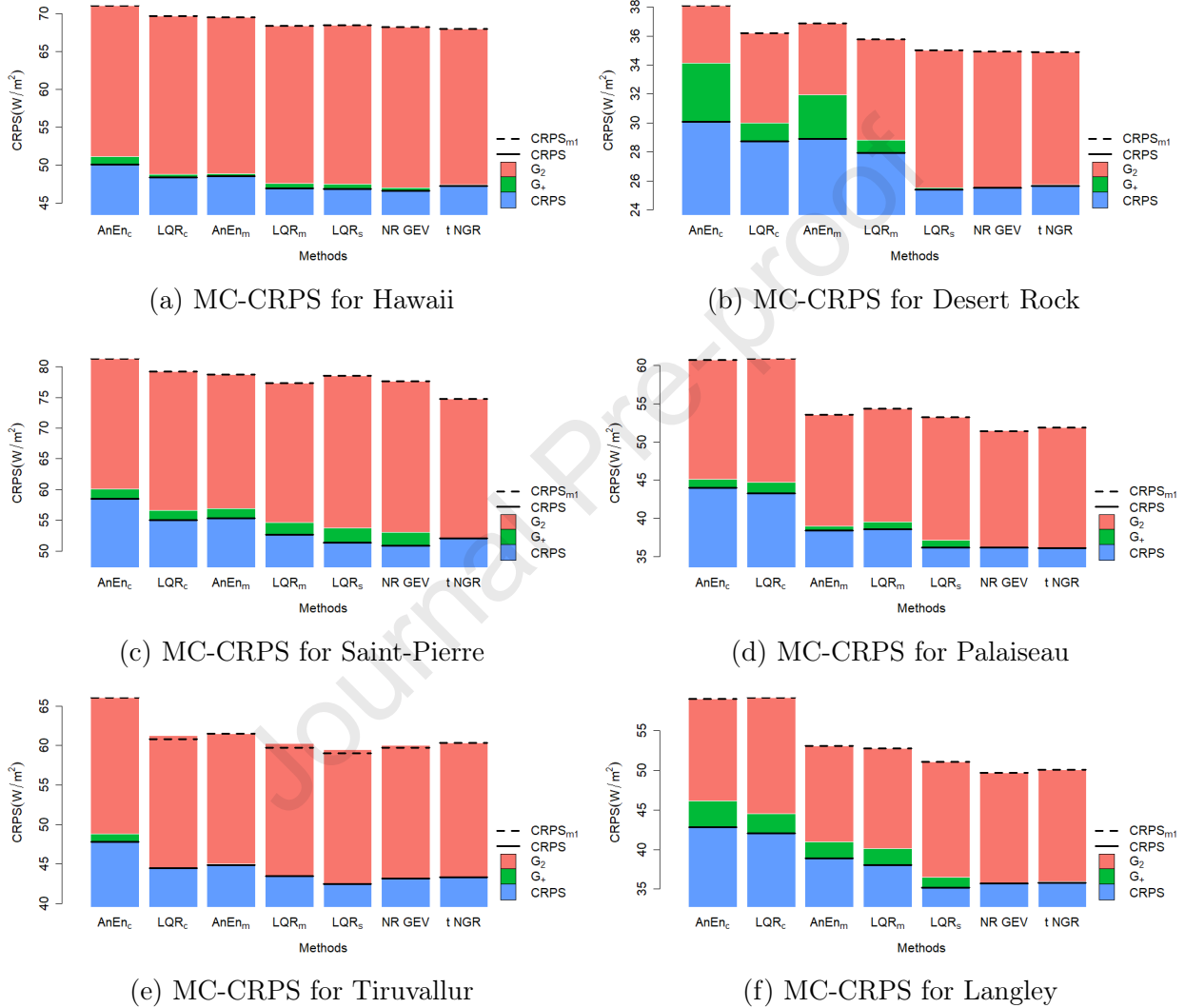


Figure 6: MC-CRPS of the six sites and all forecasting models. A black line is used to better highlight the value of the CRPS and a dotted black line indicates the value of  $CRPS_{m1}$ .

481 Figure 6 shows the results of the MC-CRPS introduced in section 3.3. As seen, the  
 482 final CRPS values, of the forecasting models occur to be dependent on their respective  
 483  $CRPS_{m1}$  values. In particular, models from the ensemble-based approach appear to have  
 484 best  $CRPS_{m1}$  than models from the deterministic-based approach (see for instance the case  
 485 of Langley). This means that the aggregation of members improves the estimation of the first



486 moment. Among the ensemble-based models, except for the cases of Hawaii and Tiruvallur,  
 487 the superiority of the  $LQR_s$ ,  $NR\_GEV$  and  $tNGR$  models using the mean and standard  
 488 deviation of the ensemble members can be mainly explained by a greater contribution of  
 489  $G_2$ . Thus the spread of EPS members is effective and improves more importantly  $G_2$  than  
 490  $CRPS_{m1}$ . Further, the best performer among the three aforementioned models is finally  
 491 determined by  $G_+$ . This highlights the importance of the choice of the distribution in the  
 492 non homogenous regression calibration framework.

493 For example, overall,  $NR\_GEV$  performs better than the  $t\_NGR$  model because of  
 494  $G_+$ . Let us stress that the choice of strictly truncated Gaussian distributions in the imple-  
 495 mentation of a  $NGR$  technique forces  $G_+$  to be very close to 0 in the MC-CRPS. Hence,  
 496 the benefits of GEV distributions compared to Gaussian distributions are highlighted by the  
 497 MC-CRPS method.

## 498 6. Discussion

499 In this section, we try to give more clues regarding the merits of each proposed approach.  
 500 Also, a discussion related to the advantages brought by the MC-CRPS is proposed.

### 501 6.1. Deterministic-based approach versus ensemble-based approach

502 Let us recall that the deterministic-based approach uses a unique deterministic predictor  
 503 while the ensemble-based approach makes use of the information conveyed by the ensemble.  
 504 Therefore, the main weakness of the deterministic-based approach is the lack of information  
 505 feeding the models. Since the distribution needs to be completely determined from one single  
 506 deterministic predictor, the spread and the possible skewness and kurtosis of the forecasting  
 507 distribution need to be only inferred from this single predictor. Conversely, the benefits  
 508 gained from the multiplicity of predictors provided by the ensemble-based approach need to  
 509 be significant to justify the computation of the EPS. Two types of benefits can be discussed.

510 First, the aggregation of predictors leads to a better estimation of the first moment.  
 511 This is visible in Figure 6 where models issued from the ensemble-based approach get better  
 512  $CRPS_{m1}$  than models from the deterministic-based approach. It is clear that a gain in the  
 513 estimation of the first moment can be obtained by the substitution of the control member  
 514 by the mean of all members.

515 Second, regarding the determination of the second moment, the uncertainty is already  
 516 carried by the level of forecasting of the mean of the EPS members. These variables are  
 517 dependent, as shown in Appendix B (the standard deviations of the observations clearly  
 518 depends on the level of forecasting). Hence, using the spread of the members of EPS as  
 519 input of the forecasting models can only be justified if it brings an extra-information on the  
 520 uncertainty. It is assumed that the spread of the members is higher if the uncertainty is so.  
 521 Indeed it indicates if slight errors in the initial conditions could lead to great differences in  
 522 the final state of the atmosphere.

523 Thus, it appears necessary to investigate on the quantity of information actually provided  
 524 by the spread of the members. In order to do this, the correlation between the standard  
 525 deviation of the observations and the spread of the members has been studied. This has been

526 made for a fixed level of forecasting, in order to remove the dependency between uncertainty  
 527 and level of forecasting. Then an average over all levels of forecasting has been calculated  
 528 to produce Figure 7. This kind of plot is of great utility to know the added value of the  
 529 standard deviation of the EPS forecast members. If the dependence between the spread of  
 530 the members and the uncertainty of the forecast for a fixed level of forecasting is strong,  
 531 then a large improvement can be expected for calibration models using the spread of the  
 532 members as an input, compared to simpler models.

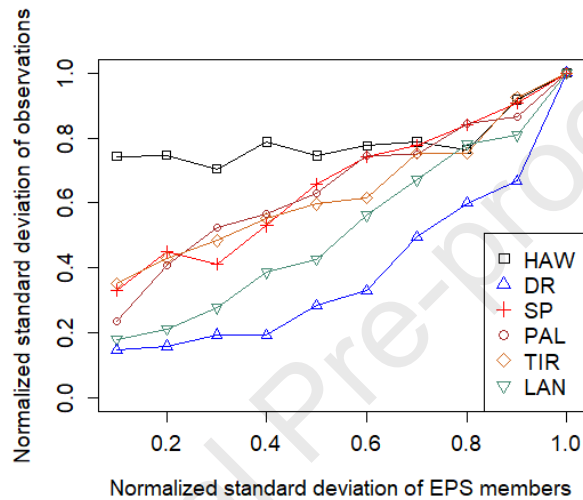


Figure 7: Standard deviation of observations vs. standard deviation of the EPS members (raw ECMWF ensembles). Normalization of the standard deviation has been done by dividing the standard deviations by the maximum of the standard deviation for each site.

533 As shown by Figure 7, the amount of new information given by the spread of the members  
 534 is very dependent on the studied site. When for Hawaii, the correlation between the standard  
 535 deviation of the observations and the spread of the members is almost null, it is quite  
 536 significant for the other sites and especially for Langley and Desert Rock. A link can be  
 537 established between this finding and Figure 5 which shows that the success of taking into  
 538 account the spread of members in the forecasting models depends on the site. It is clearly  
 539 less valuable in Hawaii than in other sites, and it is particularly successful in Desert Rock  
 540 and Langley. It is also consistent with Figure 6 where  $G_2$  is significantly higher in Desert  
 541 Rock for  $LQR_s$ ,  $t\_NGR$  and  $NR\_GEV$  models.

## 542 6.2. Discussion related to CRPS Moments-Contributions

543 In order to consolidate the results obtained in Figure 6, a complete analysis of the  
 544 statistical moments of the probability distributions produced by the forecasting methods  
 545 has been conducted. This kind of study is traditionally done to assess the strengths and  
 546 weaknesses of a forecasting model. Although the deterministic measure of a statistical  
 547 moment is not a proper scoring rule, it is of great interest to use it to understand the  
 548 behaviour of the forecasting models.

549 First, an evaluation of the accuracy of the first moment has been conducted. A good  
550 forecasting model should have the ability to give a mean value of the forecasting distributions  
551 as close as possible to the mean of the observation values. A measure of this ability can  
552 be obtained by calculating the Root Mean Square Error (RMSE) or Mean Absolute Error  
553 (MAE) of the mean of the forecasting distributions. In this study, the MAE has been  
554 chosen as it is exactly the definition of  $CRPS_{m_1}$  introduced in section 3.3 (see [38] for  
555 details). Figure 6 gives therefore the results related to the accuracy of the first moment of  
556 the distributions.

557 Second, a probabilistic forecast also provides an estimation on the level of uncertainty,  
558 which is reflected by the spread of the forecasting distribution (i.e. the second statistical  
559 moment). Some works have been specifically dedicated to the assessment of the accuracy of  
560 the spread of the predictive distributions. Among others, one can cite the studies related  
561 to the spread-skill relationship (see [48] or [49]). These works are guided by the idea that  
562 the variance of a probabilistic forecast should be larger if the uncertainty of the forecast is  
563 so. Fortin et al. [50] proposed a criterion for the evaluation of the accuracy of the second  
564 moment of the distributions. This criterion is based on the fact that statistical consistency  
565 requires that the spread of the forecasting distributions should be equal to the RMSE of the  
566 mean of the forecast. Following [50], spread is calculated as the square root of the mean  
567 of the variances of the forecasting distributions. The accuracy of the second moment is  
568 therefore measured by calculating the RMSE of the differences between spread and RMSE  
569 of the mean of the distributions (i.e.  $RMSE_M$ ). Figure 8 plots the RMSE of the difference  
570 ( $spread - RMSE_M$ ), computed over the evaluation period.

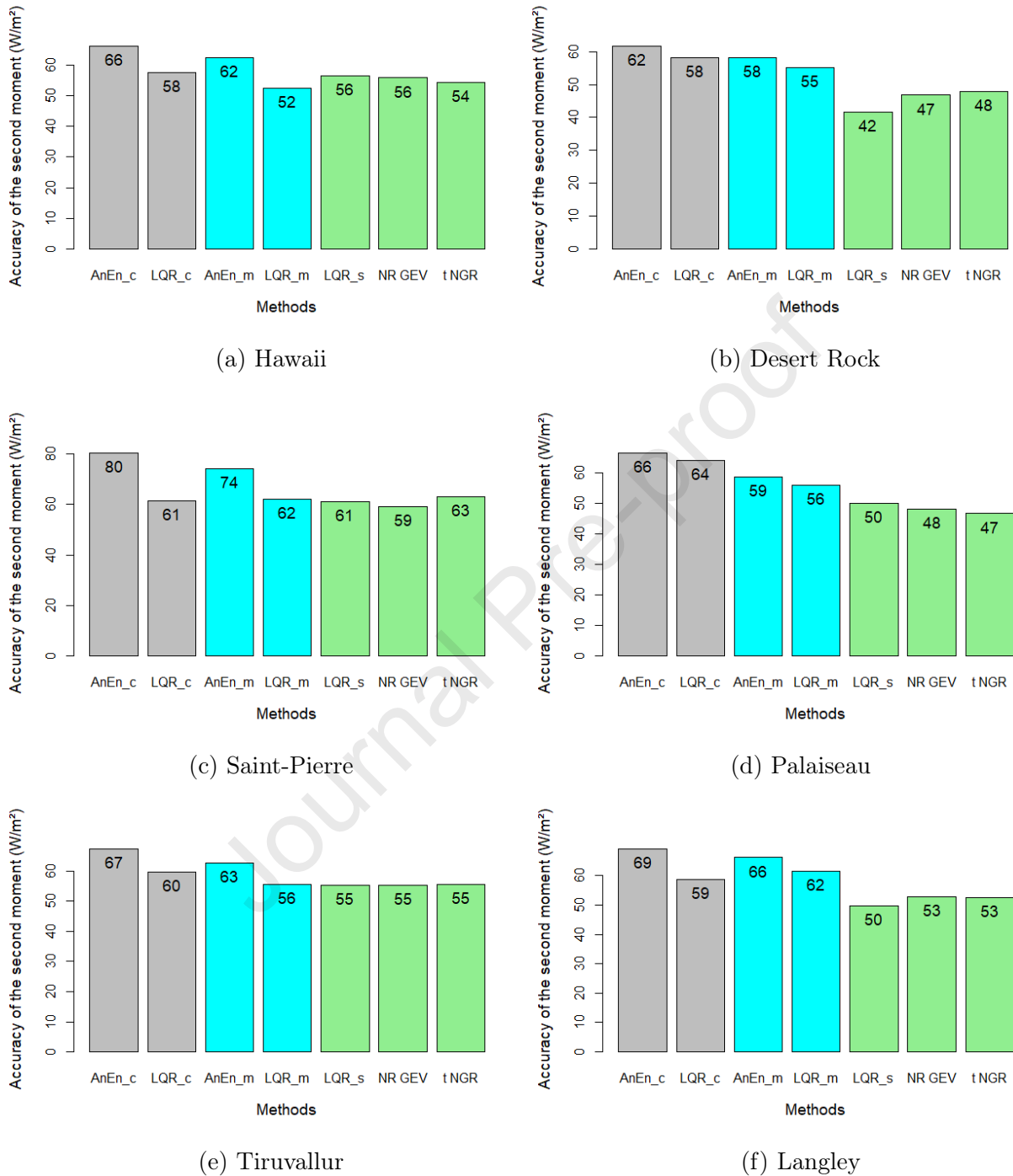
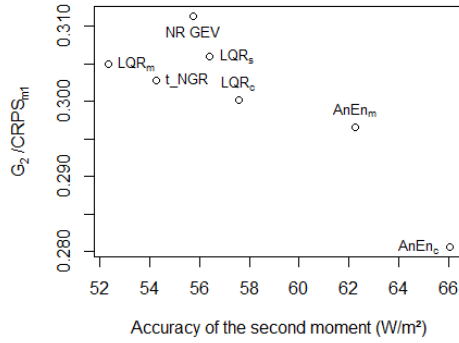


Figure 8: Accuracy of the second moment for the six studied sites and all forecasting models

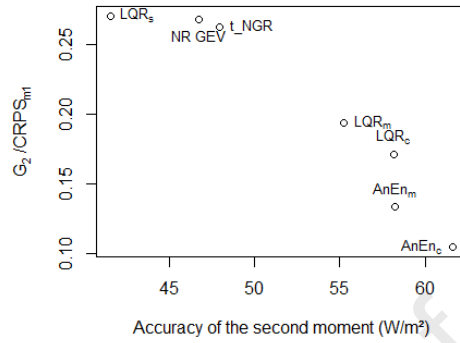
571 Conversely to the first moment, the accuracy of the second moment gradually improves  
 572 when the information taken by the forecasting model is more complete. Using the mean  
 573 of members instead of the control member increases the second moment accuracy. Taking

574 into account the spread of the EPS improves further the accuracy by approximately the  
575 same extent (except for Hawaii, for the reasons discussed in section 6.1). Nevertheless,  
576 this improvement depends on the site. As shown by Figure 8, the accuracy of the second  
577 moment for Hawaii is almost equal for each model. It is consistent with the results depicted  
578 in Figure 7, showing that the information of the second moment of the EPS distribution in  
579 Langley and Desert Rock is the most valuable, as opposed to the information of Hawaii  
580 EPS distribution.

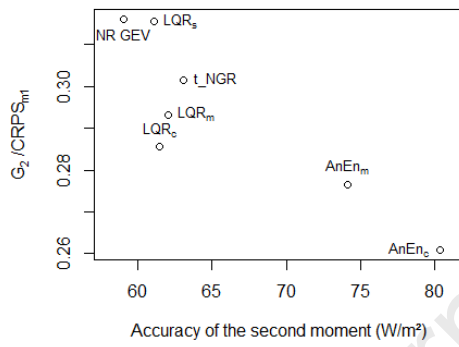
581 The accuracy of the second moment can be linked to the gain  $G_2$  introduced in the MC-  
582 CRPS section (see section 3.3). The correlation between these two values is highlighted in  
583 Figure 9, which shows the ratio  $G_2/CRPS_{m1}$  versus the accuracy of the second moment.



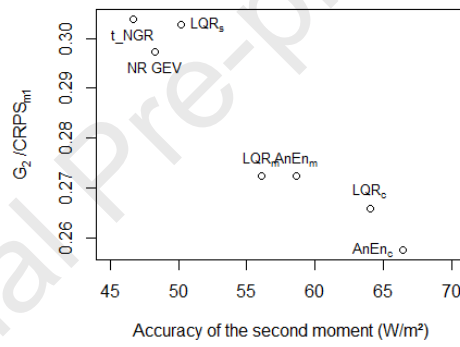
(a) Hawaii



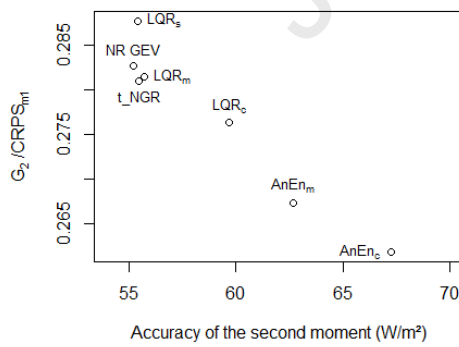
(b) Desert Rock



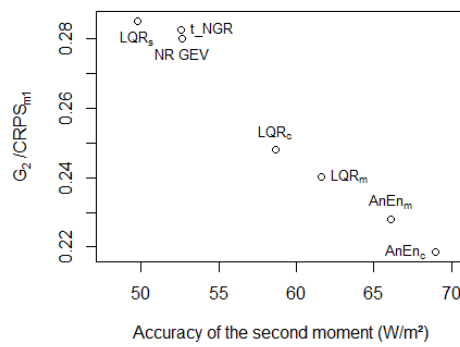
(c) Saint-Pierre



(d) Palaiseau



(e) Tiruvallur



(f) Langley

Figure 9: Link between  $G_2$  and the accuracy of the second moment.

584 To sum up, the great advantage of the MC-CRPS is to reconcile the score of a proba-  
 585 bilistic forecasting model and the explanation of its performance by examining the accuracy

586 of the moment-based distributions.

587 Moreover, the link between the calibration of the moments and the score is highlighted,  
588 because the contribution of the accuracy of the moments to the score is quantified. Here,  
589 in the proposed new diagnostic tool MC-CRPS, the accuracy of the statistical moments of  
590 the forecasting distributions is quantified by the proper score itself. This diagnostic tool  
591 is complementary of the decomposition discussed in section 3.2.3, i.e. the reliability and  
592 resolution of  $f_{m1}$  and  $f_{m2}$  can also be computed and studied. The MC-CRPS diagnostic  
593 tool also highlights the benefits of probabilistic forecasting, as the comparison between  
594  $CRPS_{m1}$  and  $CRPS$  provides a measure of the quality difference between deterministic and  
595 probabilistic forecasting.

## 596 7. Conclusions

597 Based on the two types of forecasts i.e deterministic or ensemble forecast (denoted by the  
598 term EPS for ensemble prediction system) issued by the meteorological centre ECWMF, two  
599 approaches for generating day-ahead solar irradiance probabilistic forecasts were proposed.  
600 The first approach creates probabilistic forecasts from the deterministic day-ahead GHI  
601 predictor while the second one generates probabilistic forecasts from the calibration of the  
602 EPS or from information inferred from the EPS.

603 The goal of this work was to quantify the possible added-value of the EPS on the quality  
604 of the forecasts. Six sites experiencing different sky conditions were chosen for the appraisal  
605 of the different probabilistic models. Quality of the different probabilistic models have been  
606 evaluated with common diagnostic tools such as the CRPS and its decomposition. A new  
607 diagnostic tool called MC-CRPS has also been introduced. It consists in the measure of the  
608 contribution of each statistical moment of the forecasting distributions to the CRPS.

609 Overall, models adopting the ensemble-based approach have been found to issue proba-  
610 bilistic forecasts with better quality than the ones based on the deterministic-based approach.  
611 The gain in quality, based on the CRPS metric, ranges from 4 % up to 16 %.

612 One other important contribution of this work is the new diagnostic tool related to the  
613 CRPS score based on the moments of the ensemble distribution called MC-CRPS. This  
614 MC-CRPS tool allowed to identify two characteristics of EPS that have an impact on the  
615 quality of probabilistic forecasts. First, the aggregation of deterministic predictors of the  
616 ensemble leads to an improvement of the estimation of the first moment and thus, raises the  
617 overall quality of a probabilistic forecast. Second, the spread of the EPS members turns to  
618 be a good predictor that permits to enhance the estimation of the second moment of the  
619 forecasting distributions. Finally, in terms of forecast quality, it can be concluded that using  
620 an EPS (which requires high computing capacities) to produce day-ahead GHI probabilistic  
621 forecasts should be favored compared to a deterministic (less demanding) approach. This  
622 work opens the way to the assessment of the forecast value of each approach i.e. the benefit  
623 (economical or others) gained from the use of these probabilistic forecasts in an operational  
624 context.

625 [1] M. Pierro, M. De Felice, E. Maggioni, D. Mosere, A. Perottoc, Residual load probabilistic forecast for

- 626 reserve assessment: a real case study, *Renewable Energy* 125 (2019) 99–110. doi:10.1016/j.renene.  
627 2019.12.056.
- 628 [2] Y. Zhu, Z. Toth, R. Wobus, D. Richardson, K. Mylne, The economic value of ensemble-based weather  
629 forecasts, *Bulletin of the American Meteorological Society* 83 (2002) 73–83.
- 630 [3] R. Buizza, The value of probabilistic prediction, *Atmospheric Science Letters* 9 (2008) 36–42. doi:10.  
631 1002/asl.170.
- 632 [4] M. Leutbecher, T. N. Palmer, Ensemble forecasting, *Journal of Computational Physics* 227 (2008)  
633 3515–3539. doi:10.1016/j.jcp.2007.02.014.
- 634 [5] E. Lorenz, J. Hurka, D. Heinemann, H. Beyer, Irradiance forecasting for the power prediction of grid-  
635 connected photovoltaic systems, *IEEE Journal of Selected Topics in Applied Earth Observations and*  
636 *Remote Sensing* 2 (2009) 2–10.
- 637 [6] S. Alessandrini, L. Delle Monache, S. Sperati, G. Cervone, An analog ensemble for short-term probabilis-  
638 tic solar power forecast, *Applied Energy* 157 (2015) 95–110. doi:10.1016/j.apenergy.2015.08.011.
- 639 [7] M. Zamo, O. Mestre, A. P., O. Pannekoucke, A benchmark of statistical regression methods for short-  
640 term forecasting of photovoltaic electricity production. part ii: Probabilistic forecast of daily production,  
641 *Solar Energy* 105 (2014) 804–816.
- 642 [8] P. Bacher, H. Madsen, H. A. Nielsen, Online short-term solar power forecasting, *Solar Energy*  
643 83 (2009) 1772–1783. URL: <http://linkinghub.elsevier.com/retrieve/pii/S0038092X09001364>.  
644 doi:10.1016/j.solener.2009.05.016.
- 645 [9] P. Lauret, M. David, H. Pedro, Probabilistic solar forecasting using quantile regression models, *Energies*  
646 10 (2017) 1591. doi:10.3390/en10101591.
- 647 [10] E. B. Iversen, J. M. Morales, J. K. Møller, H. Madsen, Probabilistic forecasts of solar irradiance by  
648 stochastic differential equations, *Environmetrics* 25 (2014) 152–164. doi:10.1002/env.2267.
- 649 [11] K. Bakker, K. Whan, W. Knap, M. Schmeits, Comparison of statistical post-processing methods  
650 for probabilistic nwp forecasts of solar radiation, *Solar Energy* 191 (2019) 138–150. doi:10.1016/j.  
651 solener.2019.08.044.
- 652 [12] S. Sperati, S. Alessandrini, L. Delle Monache, An application of the ecmwf ensemble prediction system  
653 for short-term solar power forecasting, *Solar Energy* 133 (2016) 437–450. doi:10.1016/j.solener.  
654 2016.04.016.
- 655 [13] L. Massidda, M. Marrocu, Quantile regression post-processing of weather forecast for short-term solar  
656 power probabilistic forecasting, *Energies* 11 (2018) 1763. doi:10.3390/en11071763.
- 657 [14] P. Pinson, Adaptive calibration of (u,v)-wind ensemble forecasts, *Quarterly Journal of the Royal*  
658 *Meteorological Society* 138 (2012) 1273–1284. doi:10.1002/qj.1873.
- 659 [15] P. Pinson, H. Madsen, Ensemble-based probabilistic forecasting at horns rev, *Wind Energy* 12 (2009)  
660 137–155. doi:10.1002/we.309.
- 661 [16] C. Junk, L. Delle Monache, S. Alessandrini, Analog-based ensemble model output statistics, *Monthly*  
662 *Weather Review* 143 (2015) 2909–2917. doi:10.1175/MWR-D-15-0095.1.
- 663 [17] T. Hamill, J. Whitaker, Probabilistic quantitative precipitation forecasts based on reforecast analogs:  
664 Theory and application, *Monthly Weather Review* 134 (2006) 3209–3229. doi:10.1175/MWR3237.1.
- 665 [18] D. S. Wilks, Comparison of ensemble-mos methods in the lorenz '96 setting, *Meteorological Applications*  
666 13 (2006) 243. doi:10.1017/S1350482706002192.
- 667 [19] R. M. Williams, C. A. T. Ferro, F. Kwasniok, A comparison of ensemble post-processing methods  
668 for extreme events, *Quarterly Journal of the Royal Meteorological Society* 140 (2014) 1112–1120.  
669 doi:10.1002/qj.2198.
- 670 [20] T. Gneiting, A. E. Raftery, A. H. Westveld, T. Goldman, Calibrated probabilistic forecasting using  
671 ensemble model output statistics and minimum crps estimation, *Monthly Weather Review* 133 (2005)  
672 1098–1118. doi:10.1175/MWR2904.1.
- 673 [21] S. Lerch, L. Thorarinsdottir, T., Comparison of non-homogeneous regression models for probabilistic  
674 wind speed forecasting, *Tellus A: Dynamic Meteorology and Oceanography* 65 (2013) 21206. doi:10.  
675 3402/tellusa.v65i0.21206.
- 676 [22] S. Baran, S. Lerch, Combining predictive distributions for the statistical post-processing of ensemble



- 677 forecasts, *International Journal of Forecasting* 34 (2018) 477–496. doi:10.1016/j.ijforecast.2018.  
678 01.005.
- 679 [23] S. Baran, S. Lerch, Log-normal distribution based emos models for probabilistic wind speed forecasting,  
680 *Quarterly Journal of the Royal Meteorological Society* 141 (2015) 2289–2299. doi:10.1002/qj.2521.
- 681 [24] S. Vannitsem, D. Wilks, J. Messner, *Statistical Postprocessing of Ensemble Forecasts*, Elsevier, 2018.
- 682 [25] P. Lauret, M. David, P. Pinson, Verification of solar irradiance probabilistic forecasts, *Solar Energy*  
683 194 (2019) 254–271. doi:10.1016/j.solener.2019.10.041.
- 684 [26] D. V. Koenker, R., Confidence intervals for regression quantiles, *Journal of the Royal Statistical Society*  
685 36 (1994) 383–393.
- 686 [27] V. Chernozhukov, I. Fernández-Val, A. Galicho, Quantile and probability curves without crossing,  
687 *Econometrica* 78 (2010) 1093–1125. doi:10.3982/ECTA7880.
- 688 [28] T. Hong, P. Pinson, S. Fan, H. Zareipour, A. Troccoli, R. Hyndman, Probabilistic energy forecasting:  
689 Global energy forecasting competition 2014 and beyond, *International Journal of Forecasting* 32 (2016)  
690 896–913. doi:10.1016/j.ijforecast.2016.02.001.
- 691 [29] L. Delle Monache, F. A. Eckel, D. Rife, B. Nagarajan, K. Searight, Probabilistic weather prediction with  
692 an analog ensemble, *Monthly Weather Review* 141 (2013) 3498–3516. doi:10.1175/MWR-D-12-00281.1.
- 693 [30] F. Calderon, J. Le Gal La Salle, J. Badosa, P. Lauret, A. Migan, V. Bourdin, Uncertainty estimation  
694 for deterministic solar irradiance forecasts based on analogs ensembles, *Renewable Energy* (2020, to be  
695 submitted).
- 696 [31] M. Scheuerer, Probabilistic quantitative precipitation forecasting using ensemble model output statis-  
697 tics: Probabilistic precipitation forecasting using emos, *Quarterly Journal of the Royal Meteorological*  
698 *Society* 140 (2014) 1086–1096. doi:10.1002/qj.2183.
- 699 [32] R. Yuen, S. Baran, C. Fraley, T. Gneiting, S. Lerch, M. Scheuerer, T. Thorarinsdottir, ensem-  
700 bleMOS: Ensemble Model Output Statistics, 2018. URL: [https://CRAN.R-project.org/package=](https://CRAN.R-project.org/package=ensembleMOS)  
701 [ensembleMOS](https://CRAN.R-project.org/package=ensembleMOS), r package version 0.8.2.
- 702 [33] S. Yitzhaki, Gini's mean difference: a superior measure of variability for non-normal distributions,  
703 *Metron - International Journal of Statistics* 61 (2003) 285–316.
- 704 [34] T. E. Hoff, R. Perez, J. Kleissl, D. Renne, J. Stein, Reporting of irradiance modeling  
705 relative prediction errors, *Progress in Photovoltaics: Research and Applications* 21 (2013)  
706 1514–1519. URL: <https://onlinelibrary.wiley.com/doi/abs/10.1002/pip.2225>. doi:10.1002/  
707 [pip.2225](https://onlinelibrary.wiley.com/doi/pdf/10.1002/pip.2225). arXiv:<https://onlinelibrary.wiley.com/doi/pdf/10.1002/pip.2225>.
- 708 [35] D. Wilks, *Statistical Methods in the Atmospheric Sciences*, Academic Press, 2014.
- 709 [36] I. T. Jolliffe, D. B. Stephenson, *Forecast Verification: A Practitioner's Guide in Atmospheric Science*,  
710 Wiley, 2003.
- 711 [37] P. Pinson, P. McSharry, H. Madsen, Reliability diagrams for non-parametric density forecasts of  
712 continuous variables: Accounting for serial correlation, *Quarterly Journal of the Royal Meteorological*  
713 *Society* 136 (2010) 77–90. URL: <http://doi.wiley.com/10.1002/qj.559>. doi:10.1002/qj.559.
- 714 [38] H. Hersbach, Decomposition of the Continuous Ranked Probability Score for Ensemble Pre-  
715 diction Systems, *Weather and Forecasting* 15 (2000) 559–570. URL: [http://journals.](http://journals.ametsoc.org/doi/abs/10.1175/1520-0434%282000%29015%3C0559%3ADOTCRP%3E2.0.CO%3B2)  
716 [ametsoc.org/doi/abs/10.1175/1520-0434%282000%29015%3C0559%3ADOTCRP%3E2.0.CO%3B2](http://journals.ametsoc.org/doi/abs/10.1175/1520-0434%282000%29015%3C0559%3ADOTCRP%3E2.0.CO%3B2).  
717 doi:10.1175/1520-0434(2000)015<0559:DOTCRP>2.0.CO;2.
- 718 [39] C. F. Coimbra, J. Kleissl, R. Marquez, Overview of Solar-Forecasting Methods and a Metric for  
719 Accuracy Evaluation, in: *Solar Energy Forecasting and Resource Assessment*, Elsevier, 2013, pp.  
720 171–194. URL: <http://linkinghub.elsevier.com/retrieve/pii/B9780123971777000085>.
- 721 [40] H. T. Pedro, C. F. Coimbra, M. David, P. Lauret, Assessment of machine learning techniques  
722 for deterministic and probabilistic intra-hour solar forecasts, *Renewable Energy* 123 (2018) 191–  
723 203. URL: <http://linkinghub.elsevier.com/retrieve/pii/S0960148118301423>. doi:10.1016/j.  
724 [renene](http://linkinghub.elsevier.com/retrieve/pii/S0960148118301423).2018.02.006.
- 725 [41] K. Doubleday, V. V. S. Hernandez], B.-M. Hodge, Benchmark probabilistic solar forecasts:  
726 Characteristics and recommendations, *Solar Energy* 206 (2020) 52 – 67. URL: [http://www.](http://www.sciencedirect.com/science/article/pii/S0038092X20305429)  
727 [sciencedirect.com/science/article/pii/S0038092X20305429](http://www.sciencedirect.com/science/article/pii/S0038092X20305429). doi:<https://doi.org/10.1016/j>.

- 728 solener.2020.05.051.
- 729 [42] J. Badosa, M. Haeffelin, H. Chepfer, Scales of spatial and temporal variation of solar irradiance on  
730 reunion tropical island, *Solar Energy* 88 (2013) 42–56. doi:10.1016/j.solener.2012.11.007.
- 731 [43] N. Kalecinski, Processus de formation et d'étalement des nuages sur l'Île de la Réunion: caractérisation  
732 à partir de données issues d'observations satellite, sol et du modèle numérique de prévision AROME;  
733 application à la prévision des énergies solaires., Ph.D. thesis, Ecole Polytechnique, 2015.
- 734 [44] T. E. Hoff, R. Perez, Modeling PV fleet output variability, *Solar Energy* 86 (2012) 2177–  
735 2189. URL: <http://linkinghub.elsevier.com/retrieve/pii/S0038092X11004154>. doi:10.1016/j.  
736 solener.2011.11.005.
- 737 [45] M. David, F. Ramahatana, P. Trombe, P. Lauret, Probabilistic forecasting of the solar irradiance with  
738 recursive ARMA and GARCH models, *Solar Energy* 133 (2016) 55–72. URL: [http://linkinghub.  
739 elsevier.com/retrieve/pii/S0038092X16300172](http://linkinghub.elsevier.com/retrieve/pii/S0038092X16300172). doi:10.1016/j.solener.2016.03.064.
- 740 [46] M. David, L. Mazorra Aguiar, P. Lauret, Comparison of intraday probabilistic forecasting of solar  
741 irradiance using only endogenous data, *International Journal of Forecasting* 34 (2018) 529–  
742 547. URL: <http://linkinghub.elsevier.com/retrieve/pii/S0169207018300384>. doi:10.1016/j.  
743 ijforecast.2018.02.003.
- 744 [47] P. Lauret, R. Perez, L. Mazorra Aguiar, E. Tapachès, H. Diagne, M. David, Characterization of  
745 the intraday variability regime of solar irradiation of climatically distinct locations, *Solar Energy*  
746 125 (2016) 99–110. URL: <https://linkinghub.elsevier.com/retrieve/pii/S0038092X15006490>.  
747 doi:10.1016/j.solener.2015.11.032.
- 748 [48] J. S. Whitaker, A. F. Loughe, The relationship between ensemble spread and ensemble mean skill,  
749 *Monthly Weather Review* 126 (1998) 3292–3302. doi:10.1175/1520-0493(1998)126<3292:TRBESA>2.  
750 0.CO;2.
- 751 [49] T. M. Hopson, Assessing the ensemble spread–error relationship, *Monthly Weather Review* 142 (2014)  
752 1125–1142. doi:10.1175/MWR-D-12-00111.1.
- 753 [50] V. Fortin, M. Abaza, F. Anctil, R. Turcotte, Why should ensemble spread match the rmse of the  
754 ensemble mean?, *Journal of Hydrometeorology* 15 (2014) 1708–1713. doi:10.1175/JHM-D-14-0008.1.
- 755 [51] C. N. Long, E. G. Dutton, BSRN Global Network recommended QC tests, V 2.0, Technical Report,  
756 PANGAEA, 2010. URL: [https://epic.awi.de/id/eprint/30083/1/BSRN\\_recommended\\_QC\\_tests\\_  
757 V2.pdf](https://epic.awi.de/id/eprint/30083/1/BSRN_recommended_QC_tests_V2.pdf).
- 758 [52] R. E. Bird, R. L. Hulstrom, Simplified Clear Sky Model for Direct and Diffuse Insolation on Horizontal  
759 Surfaces, Technical Report, Solar Energy Research Institute, Golden, CO, 1981.

## 760 Acknowledgements

761 This work benefited from the support of the Energy4Climate Interdisciplinary Center  
762 (E4C) of IP Paris and Ecole des Ponts ParisTech. It was supported by 3rd Programme  
763 d'Investissement d'Avenir (ANR-18-EUR-006-02).

## 764 Appendix A. Data quality check

A quality check has been conducted for the observation data of each of the six studied sites. As the decomposition of irradiance into diffuse and direct has not been measured, the exhaustive set of BSRN recommended quality checks could not be conducted (see [51]), but only the first plot. It consists in the plot of measured irradiance versus solar zenith angle. The rarely reached limit is plotted in dashed line and the physical possible limit is plotted in solid line. The second check is a frequency histogram of the clear-sky index ( $k^*$ )

for each site.  $k^*$  is defined as:

$$k^* = \frac{\text{Irradiance}}{\text{ClearSky Irradiance}} \quad (\text{A.1})$$

765 where the clear-sky irradiance is calculated with the Bird clear-sky model [52]. The maxi-  
 766 mum of the observed frequency is supposed to be at  $k^* = 1$ . The third check is a plot of the  
 767  $k^*$ , only for clear-sky days. The morning data is reported by black dots and afternoon data  
 768 by red dots. From this plot, it is possible to see if clear-sky irradiances are well-reported  
 769 by the measurement data. If not, the line drawn by the dots is not straight. To extract  
 770 clear-sky days from the data, the process proposed in Badosa et al. [42] has been followed.  
 771 The last figure is a plot of the  $k^*$  for each hour and day of the year. It allows to detect  
 772 if systematical biases exist at some days/hours of the year. It also allows to easily detect  
 773 missing data.

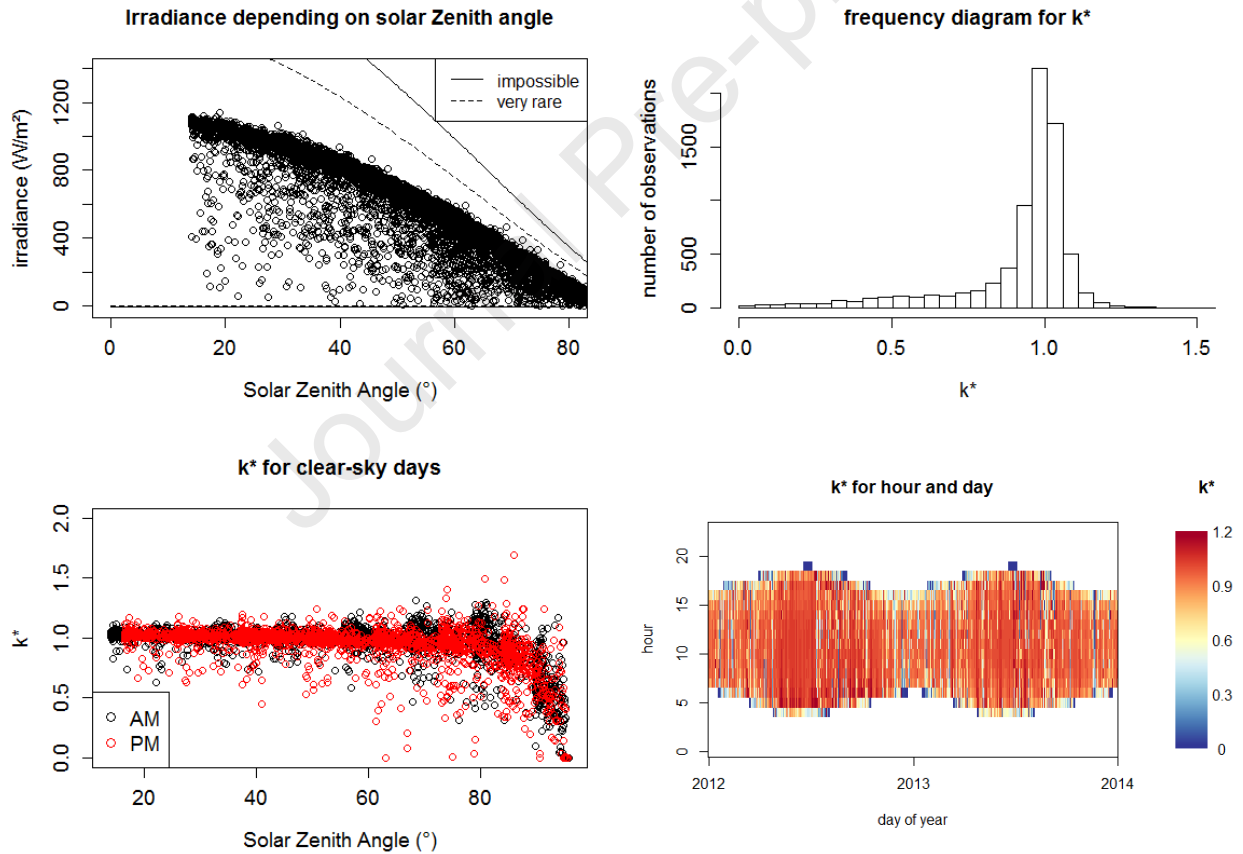


Figure A.10: Desert Rock

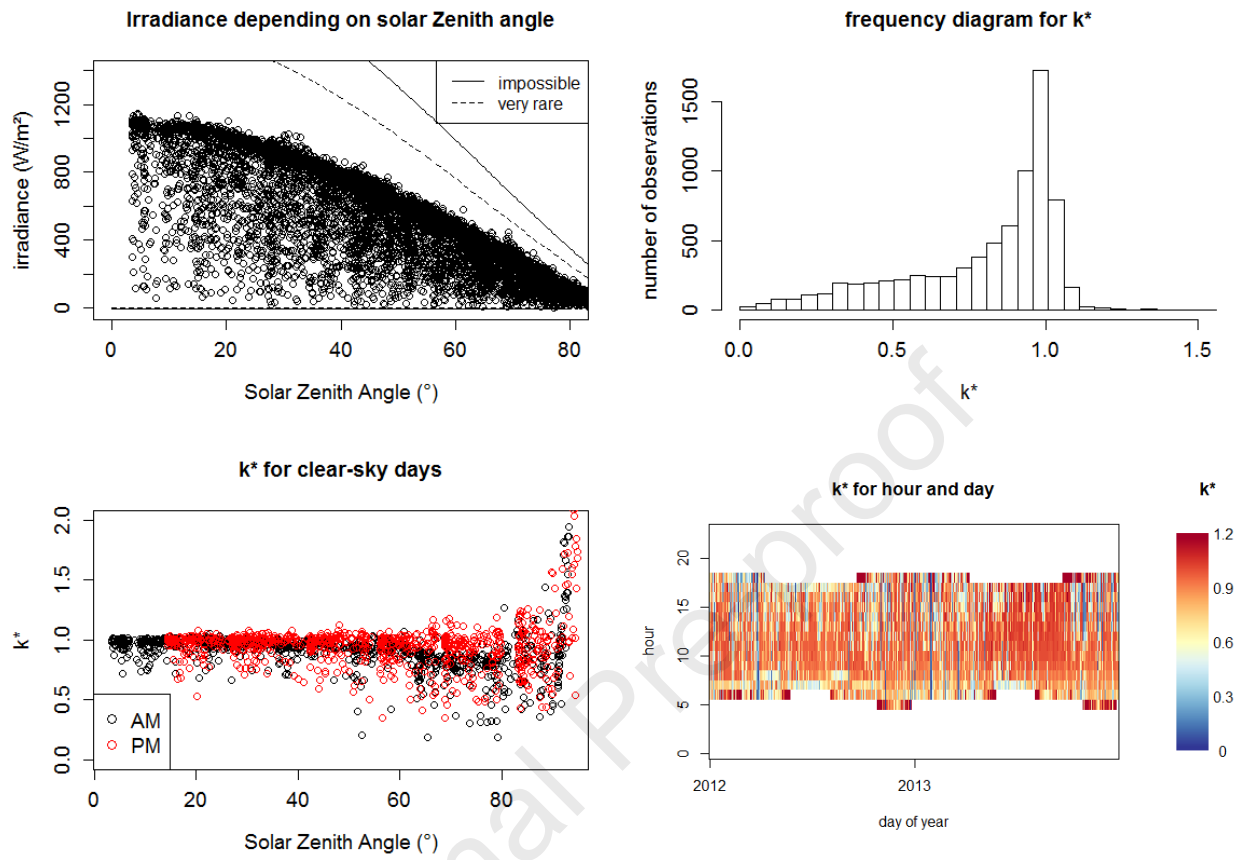


Figure A.11: Saint-Pierre

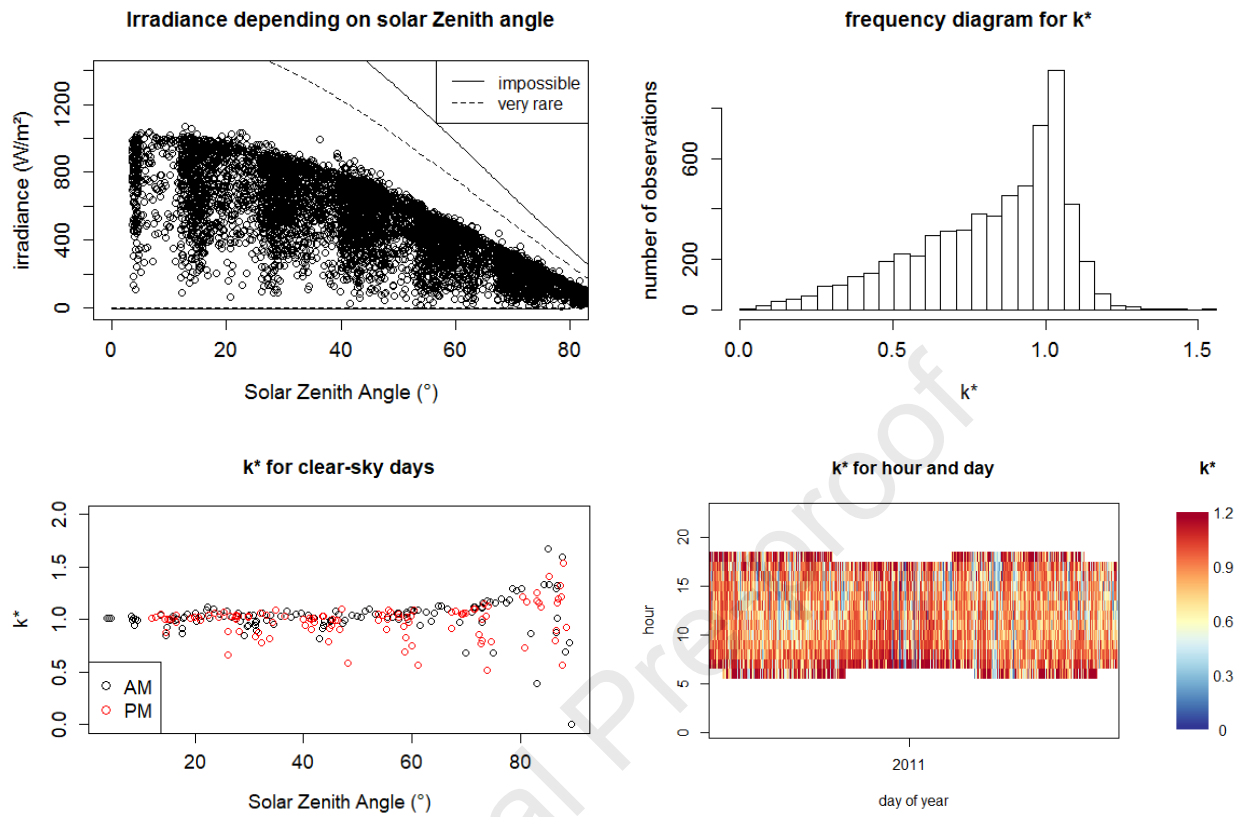


Figure A.12: Hawaii

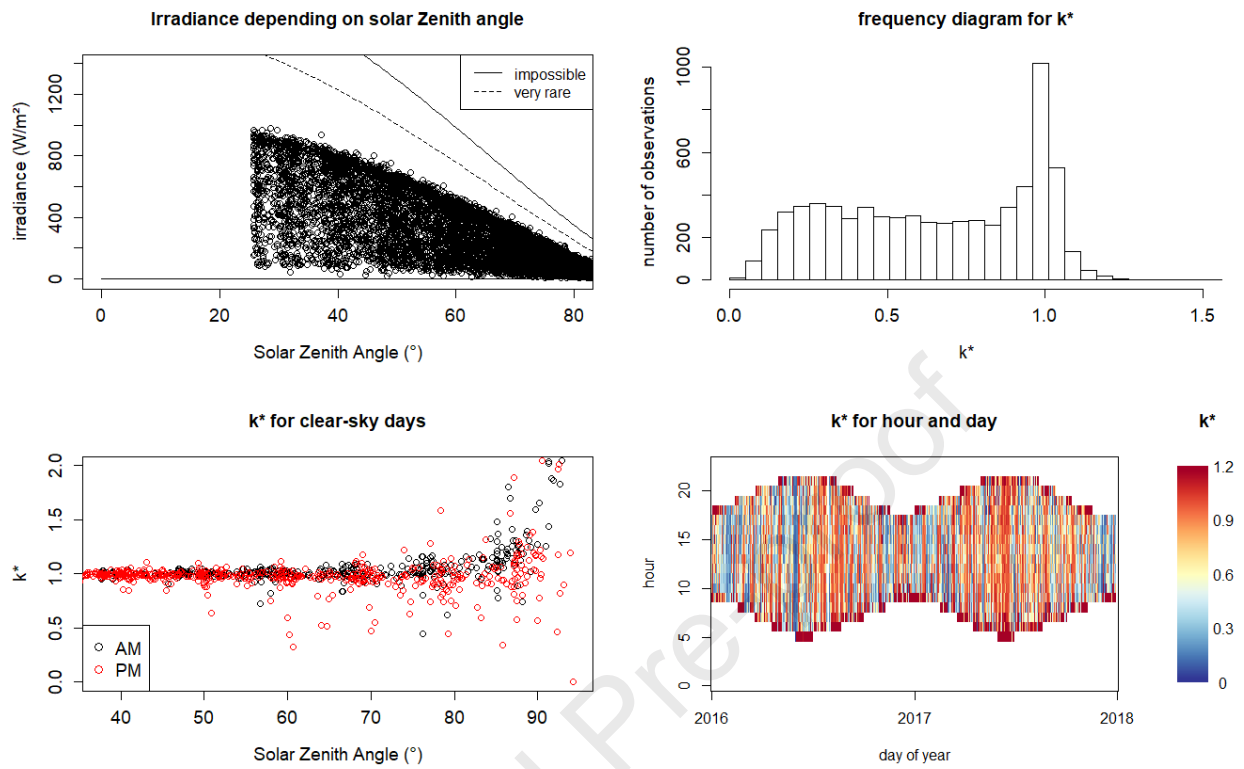


Figure A.13: Palaiseau

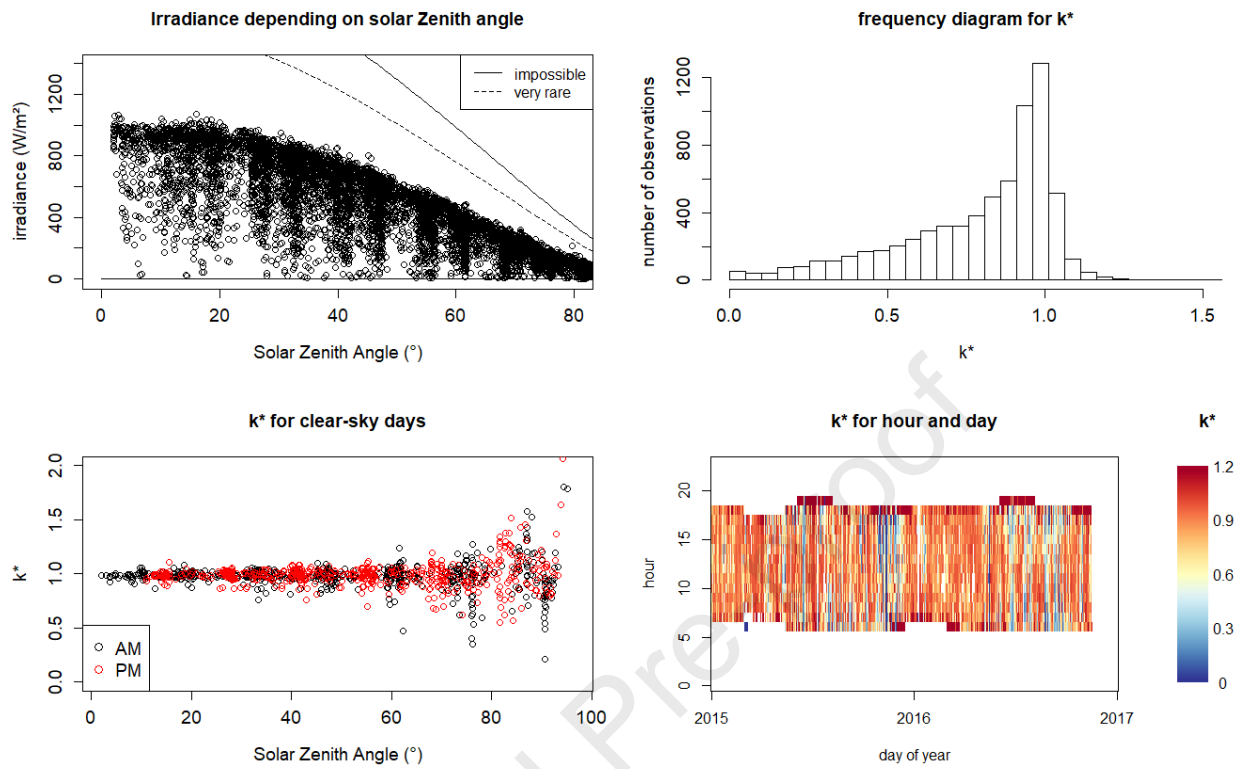


Figure A.14: Tiruvallur

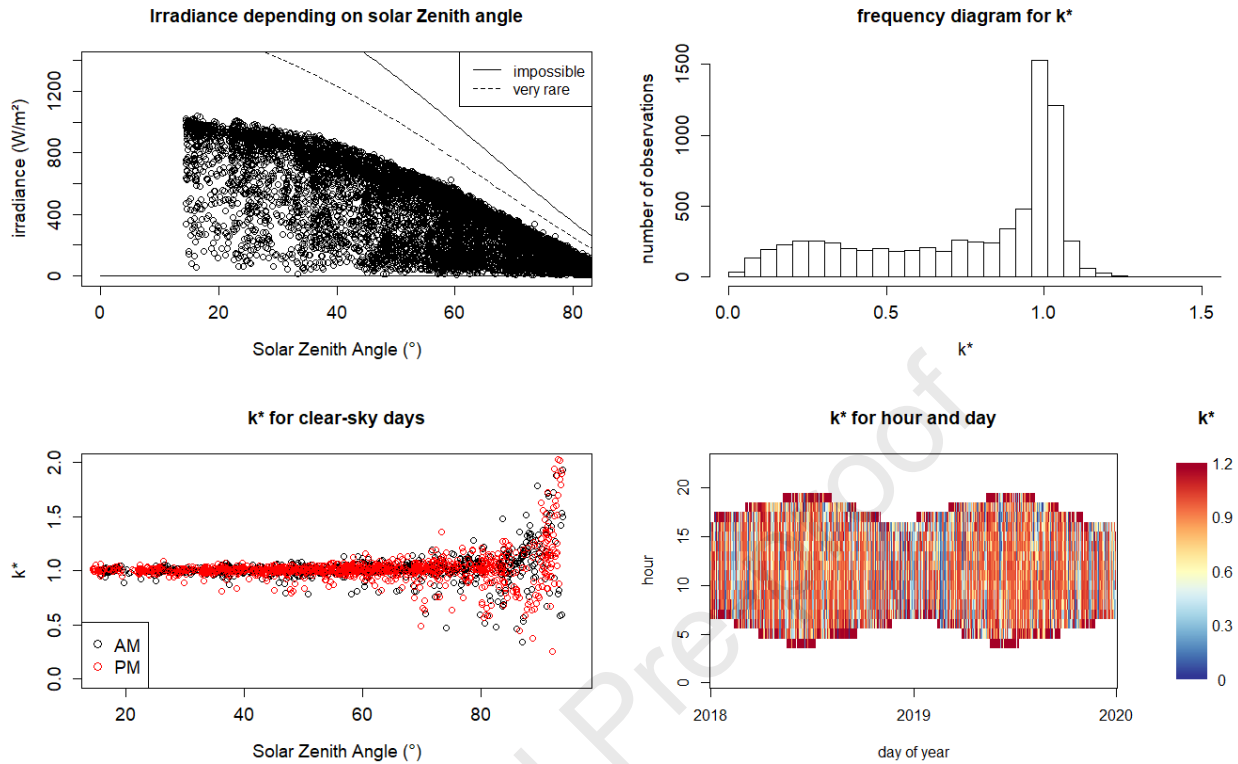


Figure A.15: Langley

774 No major issues have been detected concerning the six studied sites. For some sites  
 775 (Tiruvallur, Langley, Saint-Pierre), it is possible to guess that some reflexions occur for  
 776 extreme hours and some seasons. This leads to the phenomenon of overirradiance where  $k^*$   
 777 can easily reach a value of 4.

## 778 Appendix B. Bias and standard deviation of EPS members distribution and 779 observations for the six sites

780 The definition of the probabilistic forecast presented in section 2.3.1 is often under-  
 781 dispersive, and consequently obtains poor scores. The associated rank histograms usually  
 782 get characteristic U-shapes, with overpopulated extreme ranks. In this section, we attempt  
 783 to demonstrate why a calibration procedure is needed for raw forecasts. To this end, a  
 784 comparison between members distributions and observation distributions depending on the  
 785 level of forecasting has been conducted for the 2 first statistical moments. These plots  
 786 show clearly under-dispersive raw ensembles. The standard deviations need to be corrected.  
 787 The discrepancy between distributions of members and observations indicates a statistical  
 788 inconsistency between observations and forecasts, and therefore a bad reliability, and justifies  
 789 the use of calibration models.



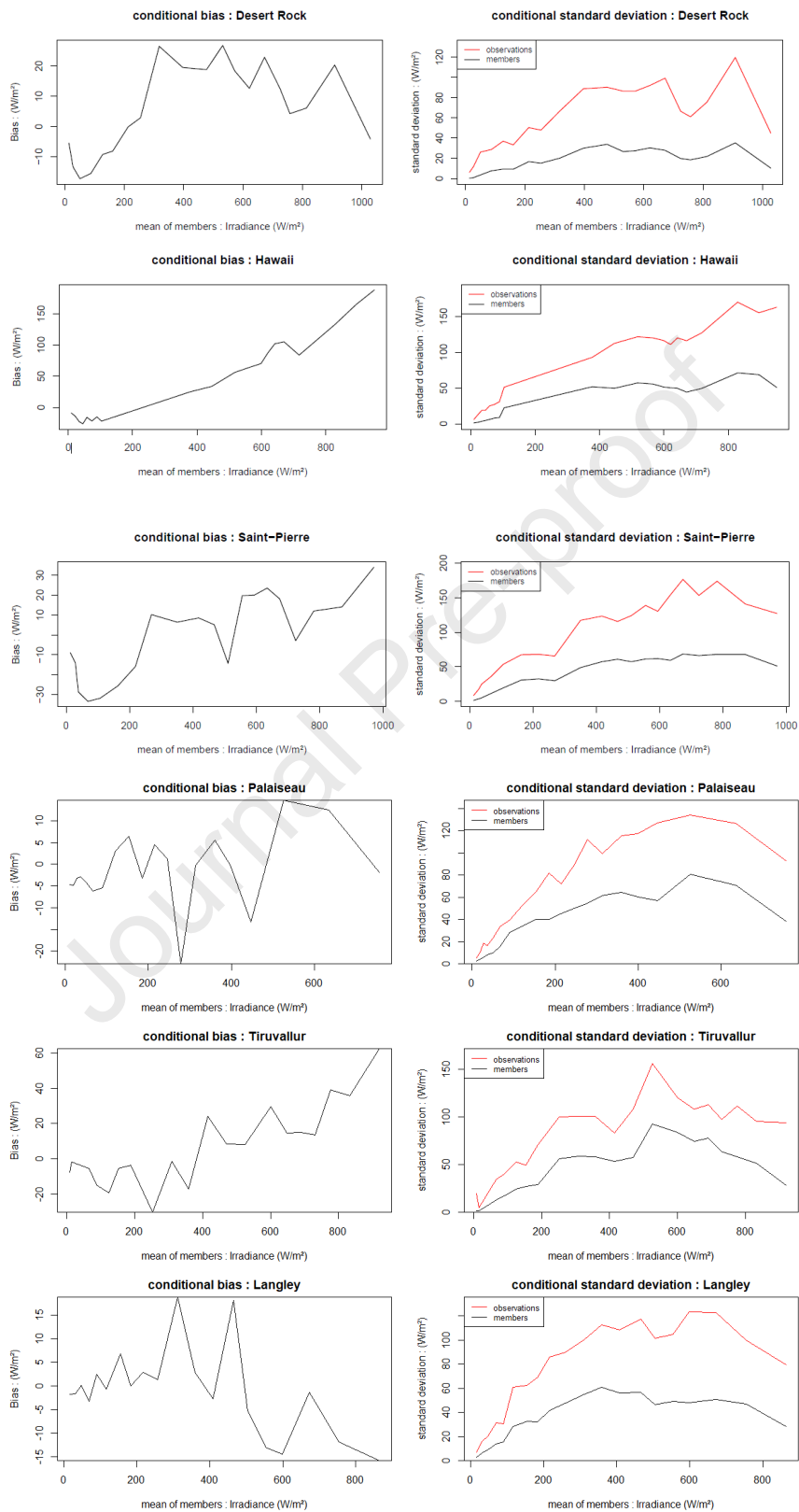


Figure B.16: Bias and standard deviation of EPS members distribution and observations for the six sites, depending on the level of forecasting

790 **Appendix C. Selection of the optimal  $\alpha$** 

791 Figure C.17 presents the results related to the optimal selection of the parameter  $\alpha$ . As  
 792 shown by Figure C.17, regardless of the site under study, the optimal value corresponds to  
 793 the minimum of the CRPS calculated on the training evaluation set.

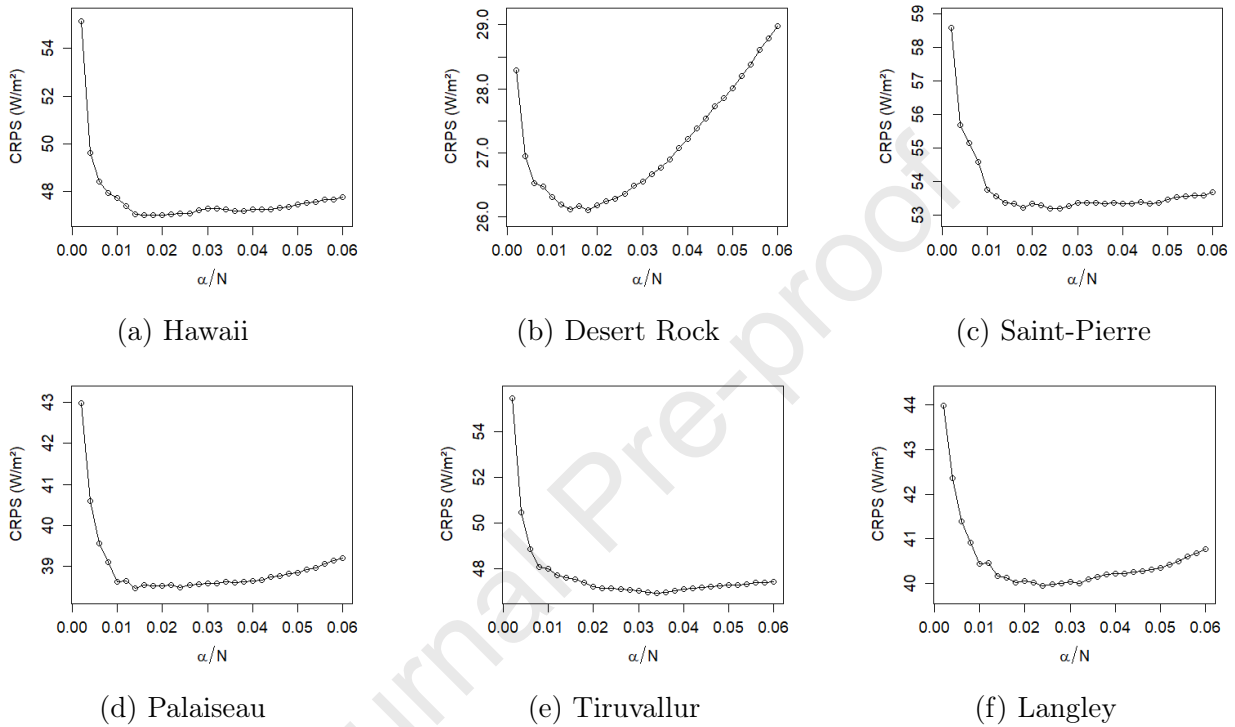


Figure C.17: Determination of the  $\alpha$ . The optimal value corresponds to the minimum of the CRPS.

- Probabilistic forecasts from deterministic informations and from Ensembles compared
- Several models either parametric and non-parametric are compared
- New tool to quantify the contributions of the statistical moments to the quality
- Sites with very different sky conditions are considered
- Using Ensemble Prediction Systems improve the quality of forecasts

Journal Pre-proof

**Declaration of interests**

The authors declare that they have no known competing financial interests or personal relationships that could have appeared to influence the work reported in this paper.

The authors declare the following financial interests/personal relationships which may be considered as potential competing interests:

Journal Pre-proof